Structural Engineering and Mechanics, *Vol. 59, No. 1 (2016) 153-186*
DOI: http://dx.doi.org/10.12989/sem.2016.59.1.153

Nonlinear higher order Reddy theory for temperature-dependent vibration and instability of embedded functionally graded pipes conveying fluid-nanoparticle mixture

M. Raminnea*, H. Biglari and F. Vakili Tahami

Faculty of Mechanical Engineering, University of Tabriz, Tabriz, Iran

(Received July 22, 2015, Revised March 29, 2016, Accepted April 15, 2016)

Abstract. This paper addresses temperature-dependent nonlinear vibration and instability of embedded functionally graded (FG) pipes conveying viscous fluid-nanoparticle mixture. The surrounding elastic medium is modeled by temperature-dependent orthotropic Pasternak medium. Reddy third-order shear deformation theory (RSDT) of cylindrical shells are developed using the strain-displacement relations of Donnell theory. The well known Navier-Stokes equation is used for obtaining the applied force of fluid to pipe. Based on energy method and Hamilton's principal, the governing equations are derived. Generalized differential quadrature method (GDQM) is applied for obtaining the frequency and critical fluid velocity of system. The effects of different parameters such as mode numbers, nonlinearity, fluid velocity, volume percent of nanoparticle in fluid, gradient index, elastic medium, boundary condition and temperature gradient are discussed. Numerical results indicate that with increasing the stiffness of elastic medium and decreasing volume percent of nanoparticle in fluid, the frequency and critical fluid velocity increase. The presented results indicate that the material in-homogeneity has a significant influence on the vibration and instability behaviors of the FG pipes and should therefore be considered in its optimum design. In addition, fluid velocity leads to divergence and flutter instabilities.

Keywords: nonlinear vibration; temperature-dependent; orthotropic pasternak medium; FG pipe; fluid-nanoparticle mixture

1. Introduction

Functionally graded materials are used in modern technologies for structural components such as those used in, nuclear, aircraft, space engineering and pressure vessels (Ng *et al*. 2001, Nguyen and Thang 2015, Kim 2015). Therefore analysis of the static and dynamic behavior of FG beam, plate and shell structures has been considered by many researchers in recent years.

The problem of dynamic behavior of plates and shells has attracted considerable attention in recent years. Reddy *et al*. (1984) studied the effect of transverse shear deformation on deflection and stresses of laminated composite plates subjected to uniformly distributed load using finite element analyses. The non-linear dynamics and stability of simply supported, circular cylindrical

*Corresponding author, Ph.D., E-mail: m.raminnia@tabrizu.ac.ir

http://www.techno-press.org/?journal=sem&subpage=8 ISSN: 1225-4568 (Print), 1598-6217 (Online)

shells containing inviscid, incompressible fluid flow was analyzed by Amabili *et al*. (2002). In another work by Amabili (2003), large-amplitude vibrations of circular cylindrical shells subjected to radial harmonic excitation in the spectral neighbourhood of the lowest resonances were investigated. Karagiozis *et al*. (2005) investigated nonlinear vibrations of circular cylindrical shells, empty or fluid-filled, clamped at both ends and subjected to a radial harmonic force excitation. The dynamics of a circular cylindrical shell carrying a rigid disk on the top and clamped at the base was investigated by Pellicano and Avramov (2007). Jansen (2008) used a perturbation method to analyze the nonlinear vibration behaviour of imperfect general structures under static preloading. Effect of geometric imperfections on non-linear stability of circular cylindrical shells conveying fluid was studied by Amabili *et al*. (2009). Dynamic stiffness matrix of an axisymmetric shell and response to harmonic distributed loads was presented by Khadimallah *et al*. (2011). Khalili *et al*. (2012) studied closed-form formulation of three-dimensional (3-D) refined higher-order shear deformation theory (RHOST) for the free vibration analysis of simply supported-simply supported and clamped-clamped homogenous isotropic circular cylindrical shells. Based on a meshless approach, postbuckling analysis of CNTR-FG cylindrical panels under axial compression was investigated by Leiw *et al*. (2014).

Functionally graded materials (FGMs) are a new generation of composite materials in which the microstructural details are spatially varied through nonuniform distribution of the reinforcement phase. The concept of FGM can be utilized for the management of a material's microstructure so that the bending behavior of a plate structure made of such material can be improved. These materials have found a wide range of applications in many industries (Shahba and Rajasekaran 2012, Wattanasakulpong *et al*. 2012). An analytical method on active vibration control of smart FG laminated cylindrical shells with thin piezoelectric layers was presented by Sheng and Wang (2009a) based on Hamilton's principle. Sheng and Wang (2009b) presented the coupling equations to govern the electric potential and the displacements of the functionally graded cylindrical shell with surface-bonded PZT piezoelectric layer, and subjected to moving loads. Considering rotary, in-plane inertias, and fluid velocity potential, the dynamic characteristics of fluid-conveying functionally graded materials (FGMs) cylindrical shells subjected to dynamic mechanical and thermal loads were investigated by Sheng and Wang (2010). A model for sigmoid FGM microplates based on the modified couple stress theory with first order shear deformation was developed by Jung *et al*. (2014). Analysis of FG carbon nanotubes reinforced plates and panels is investigated by many authors. A large deflection geometrically nonlinear behaviour of carbon nanotube-reinforced functionally graded (CNTR-FG) cylindrical panels under uniform point transverse mechanical loading was studied by Zhang *et al*. (2014a) using the kp-Ritz method. Lei *et al*. (2014) presented a first-known dynamic stability analysis of CNTR-FG cylindrical panels under static and periodic axial force by using the mesh-free kp-Ritz method. They showed the effects of different boundary conditions and types of distributions of carbon nanotubes. The effective material properties of resulting CNTR-FG panels are estimated by employing an equivalent continuum model based on the Eshelby-Mori-Tanaka approach. The analysis of flexural strength and free vibration of carbon nanotube reinforced composite cylindrical panels was carried out by Zhang *et al*. (2014b) considering four types of distributions of uniaxially aligned reinforcements. Based on a meshless approach, postbuckling analysis of CNTR-FG cylindrical panels under axial compression was investigated by Leiw *et al*. (2014). The effective material properties of CNTR-FG cylindrical panels are estimated through a micromechanical model based on the extended rule of mixture.

In the present study, nonlinear vibration and instability of temperature-dependent FG pipes

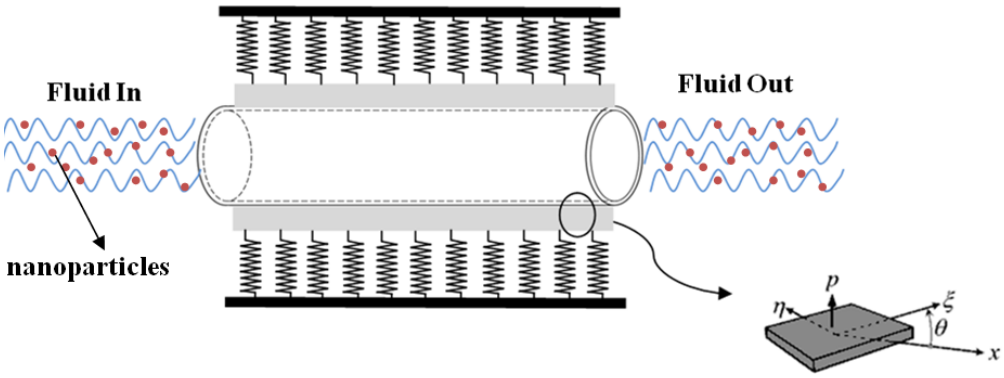

Fig. 1 Configurations of the FGM pipe resting on orthotropic elastic medium

resting on temperature-dependent orthotropic Pasternak medium are investigated. The FG pipe is conveying viscous fluid. The nonlinear governing equations are obtained based on Hamilton's principal along with Reddy shell theory. GDQM is applied for obtaining the frequency and critical fluid velocity of the FG pipe. The effects of the mode numbers, nonlinearity, fluid velocity, volume percent of nanoparticle in fluid, gradient index, Pasternak medium, temperature and boundary conditions on the frequency and critical fluid velocity of the FG pipe are disused in detail.

2. Formulation

2.1 Functionally graded materials

A schematic configuration of a FG pipe surrounded by an orthotropic elastomeric temperature-dependent medium is shown in Fig. 1. The FG pipe is often made from a mixture of two material and the composition varies continuously and smoothly in the thickness direction. Herein, the outer ($z=h/2$) and the inner ($z=-h/2$) surfaces of the FG pipe are zirconium oxide and titanium alloy, respectively.

Mechanical properties of the FG pipe including Young's modulus and mass density per unit volume are assumed to vary continuously through the pipe thickness according to either a power law distribution as (Reddy and Praveen 1998, Mirzavand and Eslami 2011)

$$E(z) = (E_z - E_t)V_c + E_t, \tag{1}$$

$$\rho(z) = (\rho_z - \rho_t)V_c + \rho_t, \tag{2}$$

in which the subscripts z and t represent the zirconium oxide and titanium alloy, respectively, and the volume fraction V_c may be given by

$$V_c = \left(\frac{z}{h} + \frac{1}{2}\right)^g, \ g \geq 0, \tag{3}$$

where g is the gradient indices and takes only positive values. For $g=0$ and $g=\infty$, the pipe is fully

zirconium oxide and titanium alloy, respectively; whereas the composition of zirconium oxide and titanium alloy is linear for g=1.

2.2 Basic equations

Based on Reddy shell theory, the displacement field can be expressed as (Reddy 1984)

$$u_x(x,\theta,z,t) = u\ (x,\theta,t) + z\psi_x(x,\theta,t) - \frac{4z^3}{3h^2}\left(\psi_x(x,\theta,t) + \frac{\partial}{\partial x} w\ (x,\theta,t)\right),$$

$$u_\theta(x,\theta,z,t) = v(x,\theta,t) + z\psi_\theta(x,\theta,t) - \frac{4z^3}{3h^2}\left(\psi_\theta(x,\theta,t) + \frac{\partial}{R\partial\theta} w\ (x,\theta,t)\right),$$

$$u_z(x,\theta,z,t) = w(x,\theta,t), \tag{4}$$

where (u_x, u_θ, u_z) denote the displacement components at an arbitrary point (x,θ,z) in the pipe, and (u,v,w) are the displacement of a material point at (x,θ) on the mid-plane (i.e., z=0) of the pipe along the x-, θ-, and z-directions, respectively; ψ_x and ψ_θ are the rotations of the normal to the mid-plane about θ- and x- directions, respectively.

The von Kármán strains associated with the above displacement field can be expressed in the following form

$$\begin{Bmatrix} \varepsilon_{xx} \\ \varepsilon_{\theta\theta} \\ \varepsilon_{x\theta} \\ \varepsilon_{xz} \\ \varepsilon_{\theta z} \end{Bmatrix} = \begin{Bmatrix} \varepsilon^0_{xx} \\ \varepsilon^0_{\theta\theta} \\ \varepsilon^0_{x\theta} \\ \varepsilon^0_{xz} \\ \varepsilon^0_{\theta z} \end{Bmatrix} + z\begin{Bmatrix} \varepsilon^1_{xx} \\ \varepsilon^1_{\theta\theta} \\ \varepsilon^1_{x\theta} \\ \varepsilon^1_{xz} \\ \varepsilon^1_{\theta z} \end{Bmatrix} + z^2\begin{Bmatrix} \varepsilon^2_{xx} \\ \varepsilon^2_{\theta\theta} \\ \varepsilon^2_{x\theta} \\ \varepsilon^2_{xz} \\ \varepsilon^2_{\theta z} \end{Bmatrix} + z^3\begin{Bmatrix} \varepsilon^3_{xx} \\ \varepsilon^3_{\theta\theta} \\ \varepsilon^3_{x\theta} \\ \varepsilon^3_{xz} \\ \varepsilon^3_{\theta z} \end{Bmatrix}, \tag{5}$$

where

$$\begin{Bmatrix} \varepsilon^0_{xx} \\ \varepsilon^0_{\theta\theta} \\ \varepsilon^0_{x\theta} \\ \varepsilon^0_{xz} \\ \varepsilon^0_{\theta z} \end{Bmatrix} = \begin{Bmatrix} \dfrac{\partial u}{\partial x} + \dfrac{1}{2}\left(\dfrac{\partial w}{\partial x}\right)^2 \\ \dfrac{\partial v}{R\partial\theta} + \dfrac{w}{R} + \dfrac{1}{2}\left(\dfrac{\partial w}{R\partial\theta}\right)^2 \\ \dfrac{\partial v}{\partial x} + \dfrac{\partial u}{R\partial\theta} + \dfrac{\partial w}{\partial x}\dfrac{\partial w}{R\partial\theta} \\ \psi_x + \dfrac{\partial w}{\partial x} \\ \psi_\theta + \dfrac{\partial w}{R\partial\theta} \end{Bmatrix}, \tag{6}$$

$$\begin{Bmatrix} \varepsilon_{xx}^{1} \\ \varepsilon_{\theta\theta}^{1} \\ \varepsilon_{x\theta}^{1} \\ \varepsilon_{xz}^{1} \\ \varepsilon_{\theta z}^{1} \end{Bmatrix} = \begin{Bmatrix} \dfrac{\partial \psi_x}{\partial x} \\ \dfrac{\partial \psi_\theta}{R\partial\theta} \\ \dfrac{\partial \psi_x}{R\partial\theta} + \dfrac{\partial \psi_\theta}{\partial x} \\ 0 \\ 0 \end{Bmatrix}, \tag{7}$$

$$\begin{Bmatrix} \varepsilon_{xx}^{2} \\ \varepsilon_{\theta\theta}^{2} \\ \varepsilon_{x\theta}^{2} \\ \varepsilon_{xz}^{2} \\ \varepsilon_{\theta z}^{2} \end{Bmatrix} = \begin{Bmatrix} 0 \\ 0 \\ 0 \\ \dfrac{-4}{h^2}\left(\psi_x + \dfrac{\partial w}{\partial x}\right) \\ \dfrac{-4}{h^2}\left(\psi_\theta + \dfrac{\partial w}{R\partial\theta}\right) \end{Bmatrix}, \tag{8}$$

$$\begin{Bmatrix} \varepsilon_{xx}^{3} \\ \varepsilon_{\theta\theta}^{3} \\ \varepsilon_{x\theta}^{3} \\ \varepsilon_{xz}^{3} \\ \varepsilon_{\theta z}^{3} \end{Bmatrix} = \begin{Bmatrix} \dfrac{-4}{3h^2}\left(\dfrac{\partial \psi_x}{\partial x} + \dfrac{\partial^2 w}{\partial x^2}\right) \\ \dfrac{-4}{3h^2}\left(\dfrac{\partial \psi_\theta}{R\partial\theta} + \dfrac{\partial^2 w}{R^2\partial\theta^2}\right) \\ \dfrac{-4}{3h^2}\left(\dfrac{\partial \psi_\theta}{\partial x} + \dfrac{\partial \psi_x}{R\partial\theta} + 2\dfrac{\partial^2 w}{R\partial x\partial\theta}\right) \\ 0 \\ 0 \end{Bmatrix}, \tag{9}$$

where (ε_{xx}, $\varepsilon_{\theta\theta}$) are the normal strain components and ($\gamma_{\theta z}$, γ_{xz}, $\gamma_{x\theta}$) are the shear strain components.

The constitutive equation for stresses $\boldsymbol{\sigma}$ and strains $\boldsymbol{\varepsilon}$ matrix in thermal environment may be written as follows

$$\begin{Bmatrix} \sigma_{xx} \\ \sigma_{\theta\theta} \\ \sigma_{\theta z} \\ \sigma_{zx} \\ \sigma_{x\theta} \end{Bmatrix} = \begin{bmatrix} C_{11}(T) & C_{12}(T) & 0 & 0 & 0 \\ C_{21}(T) & C_{22}(T) & 0 & 0 & 0 \\ 0 & 0 & C_{44}(T) & 0 & 0 \\ 0 & 0 & 0 & C_{55}(T) & 0 \\ 0 & 0 & 0 & 0 & C_{66}(T) \end{bmatrix} \begin{Bmatrix} \varepsilon_{xx} - \alpha_{xx}\Delta T \\ \varepsilon_{\theta\theta} - \alpha_{\theta\theta}\Delta T \\ \gamma_{\theta z} \\ \gamma_{xz} \\ \gamma_{x\theta} \end{Bmatrix}, \tag{10}$$

Noted that C_{ij} (i,j=1,2,...,6) and α_{xx}, $\alpha_{\theta\theta}$ may be obtained using Eqs. (1)-(3).

2.3 Energy method

The total potential energy, V, of the FG pipe is the sum of strain energy, U, kinetic energy, K, and the work done by the elasomeric medium, W.

The strain energy can be written as

$$U = \frac{1}{2}\int_{\Omega_0}\int_{-h/2}^{h/2}\left(\sigma_{xx}\varepsilon_{xx} + \sigma_{\theta\theta}\varepsilon_{\theta\theta} + \sigma_{x\theta}\gamma_{x\theta} + \sigma_{xz}\gamma_{xz} + \sigma_{\theta z}\gamma_{\theta z}\right)dV. \tag{11}$$

Combining of Eqs. (5)-(10) and (11) yields

$$\begin{aligned} U = \frac{1}{2}\int_{\Omega_0}\Bigg(& N_{xx}\left(\frac{\partial u}{\partial x} + \frac{1}{2}\left(\frac{\partial w}{\partial x}\right)^2\right) + N_{\theta\theta}\left(\frac{\partial v}{\partial \theta} + \frac{w}{R} + \frac{1}{2}\left(\frac{\partial w}{R\partial \theta}\right)^2\right) + Q_\theta\left(\frac{\partial w}{R\partial\theta} + \psi_\theta\right) \\ & + Q_x\left(\frac{\partial w}{\partial x} + \psi_x\right) + N_{x\theta}\left(\frac{\partial v}{\partial x} + \frac{\partial u}{R\partial\theta} + \frac{\partial w}{\partial x}\frac{\partial w}{R\partial\theta}\right) + M_{xx}\frac{\partial \psi_x}{\partial x} + M_{\theta\theta}\frac{\partial \psi_\theta}{R\partial\theta} + M_{x\theta}\left(\frac{\partial \psi_x}{R\partial\theta} + \frac{\partial \psi_\theta}{\partial x}\right) \\ & + K_\theta\left(\frac{-4}{h^2}\left(\psi_\theta + \frac{\partial w}{R\partial\theta}\right)\right) + K_x\left(\frac{-4}{h^2}\left(\psi_x + \frac{\partial w}{\partial x}\right)\right) + P_{xx}\left(\frac{-4}{3h^2}\left(\frac{\partial \psi_x}{\partial x} + \frac{\partial^2 w}{\partial x^2}\right)\right) \\ & + P_{\theta\theta}\left(\frac{-4}{3h^2}\left(\frac{\partial \psi_\theta}{R\partial\theta} + \frac{\partial^2 w}{R^2\partial\theta^2}\right)\right) + P_{x\theta}\left(\frac{\partial \psi_\theta}{\partial x} + \frac{\partial \psi_x}{R\partial\theta} + 2\frac{\partial^2 w}{R\partial x\partial\theta}\right)\Bigg)dx d\theta, \end{aligned} \tag{12}$$

where the stress resultant-displacement relations can be written as

$$\begin{Bmatrix} N_{xx} \\ N_{\theta\theta} \\ N_{x\theta} \end{Bmatrix} = \int_{-h/2}^{h/2}\begin{bmatrix} \sigma_{xx} \\ \sigma_{\theta\theta} \\ \sigma_{x\theta} \end{bmatrix} dz, \tag{13}$$

$$\begin{Bmatrix} M_{xx} \\ M_{\theta\theta} \\ M_{x\theta} \end{Bmatrix} = \int_{-h/2}^{h/2}\begin{bmatrix} \sigma_{xx} \\ \sigma_{\theta\theta} \\ \sigma_{x\theta} \end{bmatrix} z dz, \tag{14}$$

$$\begin{Bmatrix} P_{xx} \\ P_{\theta\theta} \\ P_{x\theta} \end{Bmatrix} = \int_{-h/2}^{h/2}\begin{bmatrix} \sigma_{xx} \\ \sigma_{\theta\theta} \\ \sigma_{x\theta} \end{bmatrix} z^3 dz, \tag{15}$$

$$\begin{bmatrix} Q_x \\ Q_\theta \end{bmatrix} = \int_{-h/2}^{h/2}\begin{bmatrix} \sigma_{xz} \\ \sigma_{\theta z} \end{bmatrix} dz, \begin{bmatrix} K_x \\ K_\theta \end{bmatrix} = \int_{-h/2}^{h/2}\begin{bmatrix} \sigma_{xz} \\ \sigma_{\theta z} \end{bmatrix} z^2 dz. \tag{16}$$

Substituting Eqs. (5)-(10) into Eqs. (13)-(16), the stress resultant-displacement relations can be obtained as follow

$$\begin{aligned} N_{xx} = {} & A_{11}\left(\frac{\partial u}{\partial x} + \frac{1}{2}\left(\frac{\partial w}{\partial x}\right)^2\right) + A_{12}\left(\frac{\partial v}{R\partial\theta} + \frac{w}{R} + \frac{1}{2}\left(\frac{\partial w}{R\partial\theta}\right)^2\right) + B_{11}\left(\frac{\partial \psi_x}{\partial x}\right) + B_{12}\left(\frac{\partial \psi_\theta}{R\partial\theta}\right) \\ & + E_{11}\left(\frac{-4}{3h^2}\left(\frac{\partial \psi_x}{\partial x} + \frac{\partial^2 w}{\partial x^2}\right)\right) + E_{12}\left(\frac{-4}{3h^2}\left(\frac{\partial \psi_\theta}{R\partial\theta} + \frac{\partial^2 w}{R^2\partial\theta^2}\right)\right) - N_{xx}^T, \end{aligned}$$

$$N_{\theta\theta} = A_{12}\left(\frac{\partial u}{\partial x}+\frac{1}{2}\left(\frac{\partial w}{\partial x}\right)^2\right)+A_{22}\left(\frac{\partial v}{R\partial\theta}+\frac{w}{R}+\frac{1}{2}\left(\frac{\partial w}{R\partial\theta}\right)^2\right)+B_{12}\left(\frac{\partial \psi_x}{\partial x}\right)+B_{22}\left(\frac{\partial \psi_\theta}{R\partial\theta}\right)$$
$$+E_{12}\left(\frac{-4}{3h^2}\left(\frac{\partial \psi_x}{\partial x}+\frac{\partial^2 w}{\partial x^2}\right)\right)+E_{22}\left(\frac{-4}{3h^2}\left(\frac{\partial \psi_\theta}{R\partial\theta}+\frac{\partial^2 w}{R^2\partial\theta^2}\right)\right)-N^T_{\theta\theta},$$
$$N_{x\theta} = A_{66}\left(\frac{\partial u}{R\partial\theta}+\frac{\partial v}{\partial x}+\frac{\partial w}{\partial x}\frac{\partial w}{R\partial\theta}\right)+B_{66}\left(\frac{\partial \psi_x}{R\partial\theta}+\frac{\partial \psi_\theta}{\partial x}\right)+E_{66}\left(\frac{-4}{3h^2}\left(\frac{\partial \psi_\theta}{\partial x}+\frac{\partial \psi_x}{R\partial\theta}+2\frac{\partial^2 w}{R\partial x\partial\theta}\right)\right), \tag{17}$$

$$M_{xx} = B_{11}\left(\frac{\partial u}{\partial x}+\frac{1}{2}\left(\frac{\partial w}{\partial x}\right)^2\right)+B_{12}\left(\frac{\partial v}{R\partial\theta}+\frac{w}{R}+\frac{1}{2}\left(\frac{\partial w}{R\partial\theta}\right)^2\right)+D_{11}\left(\frac{\partial \psi_x}{\partial x}\right)+D_{12}\left(\frac{\partial \psi_\theta}{R\partial\theta}\right)$$
$$+F_{11}\left(\frac{-4}{3h^2}\left(\frac{\partial \psi_x}{\partial x}+\frac{\partial^2 w}{\partial x^2}\right)\right)+F_{12}\left(\frac{-4}{3h^2}\left(\frac{\partial \psi_\theta}{R\partial\theta}+\frac{\partial^2 w}{R^2\partial\theta^2}\right)\right)-M^T_{xx},$$
$$M_{\theta\theta} = B_{12}\left(\frac{\partial u}{\partial x}+\frac{1}{2}\left(\frac{\partial w}{\partial x}\right)^2\right)+B_{22}\left(\frac{\partial v}{R\partial\theta}+\frac{w}{R}+\frac{1}{2}\left(\frac{\partial w}{R\partial\theta}\right)^2\right)+D_{12}\left(\frac{\partial \psi_x}{\partial x}\right)+D_{22}\left(\frac{\partial \psi_\theta}{R\partial\theta}\right) \tag{18}$$
$$+F_{12}\left(\frac{-4}{3h^2}\left(\frac{\partial \psi_x}{\partial x}+\frac{\partial^2 w}{\partial x^2}\right)\right)+F_{22}\left(\frac{-4}{3h^2}\left(\frac{\partial \psi_\theta}{R\partial\theta}+\frac{\partial^2 w}{R^2\partial\theta^2}\right)\right)-M^T_{\theta\theta},$$
$$M_{x\theta} = B_{66}\left(\frac{\partial u}{R\partial\theta}+\frac{\partial v}{\partial x}+\frac{\partial w}{\partial x}\frac{\partial w}{R\partial\theta}\right)+D_{66}\left(\frac{\partial \psi_x}{R\partial\theta}+\frac{\partial \psi_\theta}{\partial x}\right)+F_{66}\left(\frac{-4}{3h^2}\left(\frac{\partial \psi_\theta}{\partial x}+\frac{\partial \psi_x}{R\partial\theta}+2\frac{\partial^2 w}{R\partial x\partial\theta}\right)\right),$$

$$P_{xx} = E_{11}\left(\frac{\partial u}{\partial x}+\frac{1}{2}\left(\frac{\partial w}{\partial x}\right)^2\right)+E_{12}\left(\frac{\partial v}{R\partial\theta}+\frac{w}{R}+\frac{1}{2}\left(\frac{\partial w}{R\partial\theta}\right)^2\right)+F_{11}\left(\frac{\partial \psi_x}{\partial x}\right)+F_{12}\left(\frac{\partial \psi_\theta}{R\partial\theta}\right)$$
$$+H_{11}\left(\frac{-4}{3h^2}\left(\frac{\partial \psi_x}{\partial x}+\frac{\partial^2 w}{\partial x^2}\right)\right)+H_{12}\left(\frac{-4}{3h^2}\left(\frac{\partial \psi_\theta}{R\partial\theta}+\frac{\partial^2 w}{R^2\partial\theta^2}\right)\right)-P^T_{xx},$$
$$P_{\theta\theta} = E_{12}\left(\frac{\partial u}{\partial x}+\frac{1}{2}\left(\frac{\partial w}{\partial x}\right)^2\right)+E_{22}\left(\frac{\partial v}{R\partial\theta}+\frac{w}{R}+\frac{1}{2}\left(\frac{\partial w}{R\partial\theta}\right)^2\right)+F_{12}\left(\frac{\partial \psi_x}{\partial x}\right)+F_{22}\left(\frac{\partial \psi_\theta}{R\partial\theta}\right) \tag{19}$$
$$+H_{12}\left(\frac{-4}{3h^2}\left(\frac{\partial \psi_x}{\partial x}+\frac{\partial^2 w}{\partial x^2}\right)\right)+H_{22}\left(\frac{-4}{3h^2}\left(\frac{\partial \psi_\theta}{R\partial\theta}+\frac{\partial^2 w}{R^2\partial\theta^2}\right)\right)-P^T_{\theta\theta},$$
$$P_{x\theta} = E_{66}\left(\frac{\partial u}{R\partial\theta}+\frac{\partial v}{\partial x}+\frac{\partial w}{\partial x}\frac{\partial w}{R\partial\theta}\right)+F_{66}\left(\frac{\partial \psi_x}{R\partial\theta}+\frac{\partial \psi_\theta}{\partial x}\right)+H_{66}\left(\frac{-4}{3h^2}\left(\frac{\partial \psi_\theta}{\partial x}+\frac{\partial \psi_x}{R\partial\theta}+2\frac{\partial^2 w}{R\partial x\partial\theta}\right)\right),$$

$$Q_x = A_{44}\left(\frac{\partial w}{\partial x}+\psi_x\right)+D_{44}\left(\frac{-4}{h^2}\left(\psi_x+\frac{\partial w}{\partial x}\right)\right),$$
$$Q_\theta = A_{55}\left(\frac{\partial w}{R\partial\theta}+\psi_\theta\right)+D_{55}\left(\frac{-4}{h^2}\left(\psi_\theta+\frac{\partial w}{R\partial\theta}\right)\right), \tag{20}$$

$$K_x = D_{44}\left(\frac{\partial w}{\partial x}+\psi_x\right)+F_{44}\left(\frac{-4}{h^2}\left(\psi_x+\frac{\partial w}{\partial x}\right)\right),$$
$$K_\theta = D_{55}\left(\frac{\partial w}{R\partial \theta}+\psi_\theta\right)+F_{55}\left(\frac{-4}{h^2}\left(\psi_\theta+\frac{\partial w}{R\partial \theta}\right)\right), \tag{21}$$

where

$$A_{ij}=\int_{-h/2}^{h/2} C_{ij}dz, \qquad (i,j=1,2,6) \tag{22}$$

$$B_{ij}=\int_{-h/2}^{h/2} C_{ij}zdz, \tag{23}$$

$$D_{ij}=\int_{-h/2}^{h/2} C_{ij}z^2dz, \tag{24}$$

$$E_{ij}=\int_{-h/2}^{h/2} C_{ij}z^3dz, \tag{25}$$

$$F_{ij}=\int_{-h/2}^{h/2} C_{ij}z^4dz, \tag{26}$$

$$H_{ij}=\int_{-h/2}^{h/2} C_{ij}z^6dz. \tag{27}$$

Furthermore, $\left(N_{xx}^T, N_{\theta\theta}^T\right)$, $\left(M_{xx}^T, M_{\theta\theta}^T\right)$ and $\left(P_{xx}^T, P_{\theta\theta}^T\right)$ are thermal force and thermal moment resultants, respectively, and are given by

$$\begin{Bmatrix} N_{xx}^T \\ N_{\theta\theta}^T \end{Bmatrix}=\int_{-h/2}^{h/2}\begin{Bmatrix} C_{11}(T)\alpha_{xx}+C_{12}(T)\alpha_{\theta\theta} \\ C_{21}(T)\alpha_{xx}+C_{22}(T)\alpha_{\theta\theta}\end{Bmatrix}\Delta T\, dz, \tag{28}$$

$$\begin{Bmatrix} M_{xx}^T \\ M_{\theta\theta}^T \end{Bmatrix}=\int_{-h/2}^{h/2}\begin{Bmatrix} C_{11}(T)\alpha_{xx}+C_{12}(T)\alpha_{\theta\theta} \\ C_{21}(T)\alpha_{xx}+C_{22}(T)\alpha_{\theta\theta}\end{Bmatrix}\Delta T\, zdz, \tag{29}$$

$$\begin{Bmatrix} P_{xx}^T \\ P_{\theta\theta}^T \end{Bmatrix}=\int_{-h/2}^{h/2}\begin{Bmatrix} C_{11}(T)\alpha_{xx}+C_{12}(T)\alpha_{\theta\theta} \\ C_{21}(T)\alpha_{xx}+C_{22}(T)\alpha_{\theta\theta}\end{Bmatrix}\Delta T\, z^3dz. \tag{30}$$

The kinetic energy of system may be written as

$$K=\frac{\rho}{2}\int_{\Omega_0}\int_{-h/2}^{h/2}\left(\left(\dot{u}_x\right)^2+\left(\dot{u}_\theta\right)^2+\left(\dot{u}_z\right)^2\right)dV. \tag{31}$$

The external work due to Pasternak medium and fluid can be written as

$$W=\int_0^L\left(P_{Fluid}+P_{Elastic}\right)wdx. \tag{32}$$

2.4 Fluid flow work

Consider the flow of fluid in a FG pipe in which the flow is assumed to be axially symmetric, Newtonian, laminar and fully developed. The basic momentum governing equation of the flow simplifies to (Wang and Ni 2009)

$$\rho_b \frac{\partial v_r}{\partial t} = -\frac{\partial P}{\partial r} + \frac{1}{r}\frac{\partial \tau_{r\theta}}{\partial \theta} - \frac{\tau_{\theta\theta}}{r} + \frac{\partial \tau_{xr}}{\partial x}, \tag{33}$$

where ρ_b and P are fluid mass density and flow fluid pressure, respectively. The fluid force acted on the FG pipe can be calculated from Eq. (33). Since the velocity and acceleration of the pipe and fluid at the point of contact between them are equal (Wang and Ni 2009), we have

$$v_r = \frac{dw}{dt}, \tag{34}$$

where

$$\frac{d}{dt} = \frac{\partial}{\partial t} + v_x \frac{\partial}{\partial x}, \tag{35}$$

where v_x is the mean flow velocity. In Eq. (33), shear stress (τ) is dependent to viscosity $\mu_{\mu_{eff}}$ which can be expressed as follows

$$\tau_{r\theta} = \mu_{\mu_{eff}} \frac{1}{r}\frac{\partial v_r}{\partial \theta}, \tag{36a}$$

$$\tau_{\theta\theta} = 2\mu_{\mu_{eff}} \frac{v_r}{r}, \tag{36b}$$

$$\tau_{rx} = \mu_{\mu_{eff}} \frac{\partial v_r}{\partial x}. \tag{36c}$$

Finally, using Eqs. (34)-(38) and combination with Eq. (33), the fluid flow work may be written as

$$\begin{aligned} q_{Fluid} = \Bigg[& -\rho_{eff} h_f \left(\frac{\partial^2 w}{\partial t^2} + 2v_x \frac{\partial^2 w}{\partial x \partial t} + v_x^2 \frac{\partial^2 w}{\partial x^2} \right) + \frac{h_f}{R^2}\frac{\partial}{\partial \theta}\left(\mu_{eff} \left(\frac{\partial^2 w}{\partial \theta \partial t} + v_x \frac{\partial^2 w}{\partial \theta \partial x} \right) \right) \\ & - \frac{2h_f}{R}\left(\mu_{eff} \left(\frac{\partial w}{\partial t} + v_x \frac{\partial w}{\partial x} \right) \right) + h_f \frac{\partial}{\partial x}\left(\mu_{eff} \left(\frac{\partial^2 w}{\partial x \partial t} + v_x \frac{\partial^2 w}{\partial x^2} \right) \right) \Bigg], \end{aligned} \tag{37}$$

Noted that in this section, the effective viscosity ($\mu_{\mu_{eff}}$) and density ($\rho_{\mu_{eff}}$) of the fluid-nanoparticle may be calculated from mixture law as follows (Ghorbanpour Arani *et al*. 2016)

$$\rho_{eff} = \phi\rho_n + (1-\phi)\rho_f, \tag{38}$$

$$\mu_{eff} = \phi\mu_n + (1-\phi)\mu_f, \tag{39}$$

where ρ_n, ρ_f, μ_n, μ_f and ϕ are nanoparticle density, fluid density, nanoparticle viscosity, fluid viscosity and volume fraction of nanoparticle in the fluid respectively.

2.5 Orthotropic Pasternak foundation

The external force of orthotropic Pasternak medium can be expressed as (Kutlu and Omurtag 012)

$$P = K_W w - K_{g\xi}\left(\cos^2\theta\frac{\partial^2 w}{\partial x^2} + 2\cos\theta\sin\theta\frac{\partial^2 w}{R\partial x\partial\theta} + \sin^2\theta\frac{\partial^2 w}{R^2\partial\theta^2}\right) - K_{g\eta}\left(\sin^2\theta\frac{\partial^2 w}{\partial x^2} - 2\sin\theta\cos\theta\frac{\partial^2 w}{R\partial x\partial\theta} + \cos^2\theta\frac{\partial^2 w}{R^2\partial\theta^2}\right), \tag{40}$$

where K_W, $K_{g\xi}$ and $K_{g\eta}$ are spring constant of Winkler type, shear constant in ξ and η directions, respectively; angle θ describes the local ξ direction of orthotropic foundation with respect to the global x-axis of the pipe. Since the surrounding medium is relatively soft, the foundation stiffness K_W may be expressed by (Shen and Zhang 2011, Kolahchi *et al*. 2015a)

$$K_W = \frac{E_0}{4L(1-\nu_0^2)(2-c_1)^2}\left[5-\left(2\gamma_1^2+6\gamma_1+5\right)\exp\left(-2\gamma_1\right)\right], \tag{41}$$

where

$$c_1 = \left(\gamma_1+2\right)\exp\left(-\gamma_1\right), \tag{42}$$

$$\gamma_1 = \frac{H_s}{L}, \tag{43}$$

$$E_0 = \frac{E_s}{\left(1-\nu_s^2\right)}, \tag{44}$$

$$\nu_0 = \frac{\nu_s}{\left(1-\nu_s\right)}, \tag{45}$$

where E_s, ν_s, H_s are Young's modulus, Poisson's ratio and depth of the foundation, respectively. In this paper, E_s is assumed to be temperature-dependent while ν_s is assumed to be a constant.

2.6 Governing equations

The governing equations can be derived by Hamilton's principal as follows

$$\int_0^t(\delta U + \delta W - \delta K)dt = 0. \tag{46}$$

Substituting Eqs. (15) and (27) into Eq. (28) yields the following governing equations

$$\delta u: \frac{\partial N_{xx}}{\partial x} + \frac{\partial N_{x\theta}}{R\partial\theta} = I_0\frac{\partial^2 u}{\partial t^2} + J_1\frac{\partial^2\psi_x}{\partial t^2} - \frac{4I_3}{h^2}\frac{\partial^3 w}{\partial t^2\partial x}, \tag{47}$$

$$\delta v: \frac{\partial N_{x\theta}}{\partial x}+\frac{\partial N_{\theta\theta}}{R\partial\theta}=I_0\frac{\partial^2 v}{\partial t^2}+J_1\frac{\partial^2\psi_\theta}{\partial t^2}-\frac{4I_3}{h^2}\frac{\partial^3 w}{R\partial t^2\partial\theta}, \tag{48}$$

$$\begin{aligned}&\delta w: \frac{\partial Q_x}{\partial x}+\frac{\partial Q_\theta}{R\partial\theta}-\frac{4}{h^2}\left(\frac{\partial K_x}{\partial x}+\frac{\partial K_\theta}{R\partial\theta}\right)+\frac{\partial}{\partial x}\left(N_{xx}\frac{\partial w}{\partial x}+N_{x\theta}\frac{\partial w}{R\partial\theta}\right)\\&+\frac{\partial}{R\partial\theta}\left(N_{x\theta}\frac{\partial w}{\partial x}+N_{\theta\theta}\frac{\partial w}{R\partial\theta}\right)+\frac{4}{3h^2}\left(\frac{\partial^2 P_{xx}}{\partial x^2}+2\frac{\partial^2 P_{x\theta}}{R\partial x\partial\theta}+\frac{\partial^2 P_{\theta\theta}}{R^2\partial\theta^2}\right)-\frac{N_{\theta\theta}}{R}+q=\\&I_0\frac{\partial^2 w}{\partial t^2}-\left(\frac{4}{3h^2}\right)^2 I_6\left(\frac{\partial^4 w}{\partial x^2\partial t^2}+\frac{\partial^4 w}{R^2\partial\theta^2\partial t^2}\right)+\frac{4}{3h^2}\left(I_3\frac{\partial^3 u}{\partial t^2\partial x}+I_3\frac{\partial^3 v}{R\partial t^2\partial\theta}+J_4\left(\frac{\partial^3\psi_x}{\partial t^2\partial x}+\frac{\partial^3\psi_\theta}{R\partial t^2\partial\theta}\right)\right),\end{aligned} \tag{49}$$

$$\delta\psi_x: \frac{\partial M_{xx}}{\partial x}+\frac{\partial M_{x\theta}}{R\partial\theta}-\frac{4}{3h^2}\left(\frac{\partial P_{xx}}{\partial x}+\frac{\partial P_{x\theta}}{R\partial\theta}\right)-Q_x+\frac{4}{h^2}K_x=J_1\frac{\partial^2 u}{\partial t^2}+K_2\frac{\partial^2\psi_x}{\partial t^2}-\frac{4}{3h^2}J_4\frac{\partial^3 w}{\partial t^2\partial x}, \tag{50}$$

$$\delta\psi_\theta: \frac{\partial M_{x\theta}}{\partial x}+\frac{\partial M_{\theta\theta}}{R\partial\theta}-\frac{4}{3h^2}\left(\frac{\partial P_{x\theta}}{\partial x}+\frac{\partial P_{\theta\theta}}{R\partial\theta}\right)-Q_\theta+\frac{4}{h^2}K_\theta=J_1\frac{\partial^2 v}{\partial t^2}+K_2\frac{\partial^2\psi_\theta}{\partial t^2}-\frac{4}{3h^2}J_4\frac{\partial^3 w}{R\partial t^2\partial\theta}, \tag{51}$$

where

$$I_i=\int_{-h/2}^{h/2}\rho z^i dz \qquad (i=0,1,...,6), \tag{52}$$

$$J_i=I_i-\frac{4}{3h^2}I_{i+2} \qquad (i=1,4), \tag{53}$$

$$K_2=I_2-\frac{8}{3h^2}I_4+\left(\frac{4}{3h^2}\right)^2 I_6. \tag{54}$$

Substituting Eqs. (18) to (40) into Eqs. (47) to (51), the governing equations can be written as follows

$$\begin{aligned}&\delta u: \frac{\partial}{\partial x}\left(\begin{array}{l}A_{11}\left(\frac{\partial u}{\partial x}+\frac{1}{2}\left(\frac{\partial w}{\partial x}\right)^2\right)+A_{12}\left(\frac{\partial v}{R\partial\theta}+\frac{w}{R}+\frac{1}{2}\left(\frac{\partial w}{R\partial\theta}\right)^2\right)+B_{11}\left(\frac{\partial\psi_x}{\partial x}\right)+B_{12}\left(\frac{\partial\psi_\theta}{R\partial\theta}\right)\\+E_{11}\left(\frac{-4}{3h^2}\left(\frac{\partial\psi_x}{\partial x}+\frac{\partial^2 w}{\partial x^2}\right)\right)+E_{12}\left(\frac{-4}{3h^2}\left(\frac{\partial\psi_\theta}{R\partial\theta}+\frac{\partial^2 w}{R^2\partial\theta^2}\right)\right)\end{array}\right)\\&+\frac{\partial}{R\partial\theta}\left(A_{66}\left(\frac{\partial u}{R\partial\theta}+\frac{\partial v}{\partial x}+\frac{\partial w}{\partial x}\frac{\partial w}{R\partial\theta}\right)+B_{66}\left(\frac{\partial\psi_x}{R\partial\theta}+\frac{\partial\psi_\theta}{\partial x}\right)+E_{66}\left(\frac{-4}{3h^2}\left(\frac{\partial\psi_\theta}{\partial x}+\frac{\partial\psi_x}{R\partial\theta}+2\frac{\partial^2 w}{R\partial x\partial\theta}\right)\right)\right)\\&=I_0\frac{\partial^2 u}{\partial t^2}+J_1\frac{\partial^2\psi_x}{\partial t^2}-\frac{4I_3}{h^2}\frac{\partial^3 w}{\partial t^2\partial x},\end{aligned} \tag{55}$$

$$
\begin{aligned}
&\delta v: \frac{\partial}{R\partial\theta}\left(\begin{array}{l} A_{12}\left(\frac{\partial u}{\partial x}+\frac{1}{2}\left(\frac{\partial w}{\partial x}\right)^2\right)+A_{22}\left(\frac{\partial v}{R\partial\theta}+\frac{w}{R}+\frac{1}{2}\left(\frac{\partial w}{R\partial\theta}\right)^2\right)+B_{12}\left(\frac{\partial \psi_x}{\partial x}\right)+B_{22}\left(\frac{\partial \psi_\theta}{R\partial\theta}\right) \\ +E_{12}\left(\frac{-4}{3h^2}\left(\frac{\partial \psi_x}{\partial x}+\frac{\partial^2 w}{\partial x^2}\right)\right)+E_{22}\left(\frac{-4}{3h^2}\left(\frac{\partial \psi_\theta}{R\partial\theta}+\frac{\partial^2 w}{R^2\partial\theta^2}\right)\right)\end{array}\right) \\
&+\frac{\partial}{\partial x}\left(A_{66}\left(\frac{\partial u}{R\partial\theta}+\frac{\partial v}{\partial x}+\frac{\partial w}{\partial x}\frac{\partial w}{R\partial\theta}\right)+B_{66}\left(\frac{\partial \psi_x}{R\partial\theta}+\frac{\partial \psi_\theta}{\partial x}\right)+E_{66}\left(\frac{-4}{3h^2}\left(\frac{\partial \psi_\theta}{\partial x}+\frac{\partial \psi_x}{R\partial\theta}+2\frac{\partial^2 w}{R\partial x\partial\theta}\right)\right)\right) \\
&=I_0\frac{\partial^2 v}{\partial t^2}+J_1\frac{\partial^2 \psi_\theta}{\partial t^2}-\frac{4I_3}{h^2}\frac{\partial^3 w}{R\partial t^2\partial\theta},
\end{aligned}
\tag{56}
$$

$$
\begin{aligned}
&\delta w: \frac{\partial}{\partial x}\left(A_{44}\left(\frac{\partial w}{\partial x}+\psi_x\right)+D_{44}\left(\frac{-4}{h^2}\left(\psi_x+\frac{\partial w}{\partial x}\right)\right)\right)+\frac{\partial}{R\partial\theta}\left(A_{55}\left(\frac{\partial w}{R\partial\theta}+\psi_\theta\right)+D_{55}\left(\frac{-4}{h^2}\left(\psi_\theta+\frac{\partial w}{R\partial\theta}\right)\right)\right) \\
&+\frac{\partial}{\partial x}\left(N_{xx}\frac{\partial w}{\partial x}+N_{x\theta}\frac{\partial w}{R\partial\theta}\right)+\frac{\partial}{R\partial\theta}\left(N_{x\theta}\frac{\partial w}{\partial x}+N_{\theta\theta}\frac{\partial w}{R\partial\theta}\right) \\
&-\frac{4}{h^2}\left(\frac{\partial}{\partial x}\left(D_{44}\left(\frac{\partial w}{\partial x}+\psi_x\right)+F_{44}\left(\frac{-4}{h^2}\left(\psi_x+\frac{\partial w}{\partial x}\right)\right)\right)+\frac{\partial}{R\partial\theta}\left(D_{55}\left(\frac{\partial w}{R\partial\theta}+\psi_\theta\right)+F_{55}\left(\frac{-4}{h^2}\left(\psi_\theta+\frac{\partial w}{R\partial\theta}\right)\right)\right)\right) \\
&+\frac{\partial^2}{\partial x^2}\left(\begin{array}{l} E_{11}\left(\frac{\partial u}{\partial x}+\frac{1}{2}\left(\frac{\partial w}{\partial x}\right)^2\right)+E_{12}\left(\frac{\partial v}{R\partial\theta}+\frac{w}{R}+\frac{1}{2}\left(\frac{\partial w}{R\partial\theta}\right)^2\right)+F_{11}\left(\frac{\partial \psi_x}{\partial x}\right)+F_{12}\left(\frac{\partial \psi_\theta}{R\partial\theta}\right) \\ +H_{11}\left(\frac{-4}{3h^2}\left(\frac{\partial \psi_x}{\partial x}+\frac{\partial^2 w}{\partial x^2}\right)\right)+H_{12}\left(\frac{-4}{3h^2}\left(\frac{\partial \psi_\theta}{R\partial\theta}+\frac{\partial^2 w}{R^2\partial\theta^2}\right)\right)\end{array}\right) \\
&+\frac{4}{3h^2}\left(\begin{array}{l} +2\frac{\partial^2}{R\partial x\partial\theta}\left(\begin{array}{l} E_{66}\left(\frac{\partial u}{R\partial\theta}+\frac{\partial v}{\partial x}+\frac{\partial w}{\partial x}\frac{\partial w}{R\partial\theta}\right)+F_{66}\left(\frac{\partial \psi_x}{R\partial\theta}+\frac{\partial \psi_\theta}{\partial x}\right) \\ +H_{66}\left(\frac{-4}{3h^2}\left(\frac{\partial \psi_\theta}{\partial x}+\frac{\partial \psi_x}{R\partial\theta}+2\frac{\partial^2 w}{R\partial x\partial\theta}\right)\right)\end{array}\right) \\ +\frac{\partial^2}{R^2\partial\theta^2}\left(\begin{array}{l} E_{12}\left(\frac{\partial u}{\partial x}+\frac{1}{2}\left(\frac{\partial w}{\partial x}\right)^2\right)+E_{22}\left(\frac{\partial v}{R\partial\theta}+\frac{w}{R}+\frac{1}{2}\left(\frac{\partial w}{R\partial\theta}\right)^2\right)+F_{12}\left(\frac{\partial \psi_x}{\partial x}\right)+F_{22}\left(\frac{\partial \psi_\theta}{R\partial\theta}\right) \\ +H_{12}\left(\frac{-4}{3h^2}\left(\frac{\partial \psi_x}{\partial x}+\frac{\partial^2 w}{\partial x^2}\right)\right)+H_{22}\left(\frac{-4}{3h^2}\left(\frac{\partial \psi_\theta}{R\partial\theta}+\frac{\partial^2 w}{R^2\partial\theta^2}\right)\right)\end{array}\right)\end{array}\right) \\
&-\frac{1}{R}\left(\begin{array}{l} A_{12}\left(\frac{\partial u}{\partial x}+\frac{1}{2}\left(\frac{\partial w}{\partial x}\right)^2\right)+A_{22}\left(\frac{\partial v}{R\partial\theta}+\frac{w}{R}+\frac{1}{2}\left(\frac{\partial w}{R\partial\theta}\right)^2\right)+B_{12}\left(\frac{\partial \psi_x}{\partial x}\right)+B_{22}\left(\frac{\partial \psi_\theta}{R\partial\theta}\right) \\ +E_{12}\left(\frac{-4}{3h^2}\left(\frac{\partial \psi_x}{\partial x}+\frac{\partial^2 w}{\partial x^2}\right)\right)+E_{22}\left(\frac{-4}{3h^2}\left(\frac{\partial \psi_\theta}{R\partial\theta}+\frac{\partial^2 w}{R^2\partial\theta^2}\right)\right)\end{array}\right) \\
&+K_W w-K_{g\xi}\left(\cos^2\theta\frac{\partial^2 w}{\partial x^2}+2\cos\theta\sin\theta\frac{\partial^2 w}{R\partial x\partial\theta}+\sin^2\theta\frac{\partial^2 w}{R^2\partial\theta^2}\right) \\
&-K_{g\eta}\left(\sin^2\theta\frac{\partial^2 w}{\partial x^2}-2\sin\theta\cos\theta\frac{\partial^2 w}{R\partial x\partial\theta}+\cos^2\theta\frac{\partial^2 w}{R^2\partial\theta^2}\right)+\left[-\rho_f h_f\left(\frac{\partial^2 w}{\partial t^2}+2v_x\frac{\partial^2 w}{\partial x\partial t}+v_x^2\frac{\partial^2 w}{\partial x^2}\right)\right.
\end{aligned}
$$

$$+\frac{h_f}{R^2}\frac{\partial}{\partial\theta}\left(\mu\left(\frac{\partial^2 w}{\partial\theta\partial t}+v_x\frac{\partial^2 w}{\partial\theta\partial x}\right)\right)-\frac{2h_f}{R}\left(\mu\left(\frac{\partial w}{\partial t}+v_x\frac{\partial w}{\partial x}\right)\right)+h_f\frac{\partial}{\partial x}\left(\mu\left(\frac{\partial^2 w}{\partial x\partial t}+v_x\frac{\partial^2 w}{\partial x^2}\right)\right)\Bigg]$$
$$=I_0\frac{\partial^2 w}{\partial t^2}-\left(\frac{4}{3h^2}\right)^2 I_6\left(\frac{\partial^4 w}{\partial x^2\partial t^2}+\frac{\partial^4 w}{R^2\partial\theta^2\partial t^2}\right)+\frac{4}{3h^2}\left(I_3\frac{\partial^3 u}{\partial t^2\partial x}+I_3\frac{\partial^3 v}{R\partial t^2\partial\theta}+J_4\left(\frac{\partial^3\psi_x}{\partial t^2\partial x}+\frac{\partial^3\psi_\theta}{R\partial t^2\partial\theta}\right)\right), \tag{57}$$

$$\delta\psi_x:\frac{\partial}{\partial x}\left(\begin{array}{l}B_{11}\left(\frac{\partial u}{\partial x}+\frac{1}{2}\left(\frac{\partial w}{\partial x}\right)^2\right)+B_{12}\left(\frac{\partial v}{R\partial\theta}+\frac{w}{R}+\frac{1}{2}\left(\frac{\partial w}{R\partial\theta}\right)^2\right)+D_{11}\left(\frac{\partial\psi_x}{\partial x}\right)+D_{12}\left(\frac{\partial\psi_\theta}{R\partial\theta}\right)\\+F_{11}\left(\frac{-4}{3h^2}\left(\frac{\partial\psi_x}{\partial x}+\frac{\partial^2 w}{\partial x^2}\right)\right)+F_{12}\left(\frac{-4}{3h^2}\left(\frac{\partial\psi_\theta}{R\partial\theta}+\frac{\partial^2 w}{R^2\partial\theta^2}\right)\right)\end{array}\right)$$
$$+\frac{\partial}{R\partial\theta}\left(B_{66}\left(\frac{\partial u}{R\partial\theta}+\frac{\partial v}{\partial x}+\frac{\partial w}{\partial x}\frac{\partial w}{R\partial\theta}\right)+D_{66}\left(\frac{\partial\psi_x}{R\partial\theta}+\frac{\partial\psi_\theta}{\partial x}\right)+F_{66}\left(\frac{-4}{3h^2}\left(\frac{\partial\psi_\theta}{\partial x}+\frac{\partial\psi_x}{R\partial\theta}+2\frac{\partial^2 w}{R\partial x\partial\theta}\right)\right)\right)$$
$$-A_{44}\left(\frac{\partial w}{\partial x}+\psi_x\right)-D_{44}\left(\frac{-4}{h^2}\left(\psi_x+\frac{\partial w}{\partial x}\right)\right)+\frac{4}{h^2}\left(D_{44}\left(\frac{\partial w}{\partial x}+\psi_x\right)+F_{44}\left(\frac{-4}{h^2}\left(\psi_x+\frac{\partial w}{\partial x}\right)\right)\right)$$
$$-\frac{4}{3h^2}\left(\begin{array}{l}\frac{\partial}{\partial x}\left(\begin{array}{l}E_{11}\left(\frac{\partial u}{\partial x}+\frac{1}{2}\left(\frac{\partial w}{\partial x}\right)^2\right)+E_{12}\left(\frac{\partial v}{R\partial\theta}+\frac{w}{R}+\frac{1}{2}\left(\frac{\partial w}{R\partial\theta}\right)^2\right)+F_{11}\left(\frac{\partial\psi_x}{\partial x}\right)+F_{12}\left(\frac{\partial\psi_\theta}{R\partial\theta}\right)\\+H_{11}\left(\frac{-4}{3h^2}\left(\frac{\partial\psi_x}{\partial x}+\frac{\partial^2 w}{\partial x^2}\right)\right)+H_{12}\left(\frac{-4}{3h^2}\left(\frac{\partial\psi_\theta}{R\partial\theta}+\frac{\partial^2 w}{R^2\partial\theta^2}\right)\right)\end{array}\right)\\+\frac{\partial}{R\partial\theta}\left(\begin{array}{l}E_{66}\left(\frac{\partial u}{R\partial\theta}+\frac{\partial v}{\partial x}+\frac{\partial w}{\partial x}\frac{\partial w}{R\partial\theta}\right)+F_{66}\left(\frac{\partial\psi_x}{R\partial\theta}+\frac{\partial\psi_\theta}{\partial x}\right)\\+H_{66}\left(\frac{-4}{3h^2}\left(\frac{\partial\psi_\theta}{\partial x}+\frac{\partial\psi_x}{R\partial\theta}+2\frac{\partial^2 w}{R\partial x\partial\theta}\right)\right)\end{array}\right)\end{array}\right)$$
$$=J_1\frac{\partial^2 u}{\partial t^2}+K_2\frac{\partial^2\psi_x}{\partial t^2}-\frac{4}{3h^2}J_4\frac{\partial^3 w}{\partial t^2\partial x}, \tag{58}$$

$$\delta\psi_\theta:\frac{\partial}{\partial x}\left(B_{66}\left(\frac{\partial u}{R\partial\theta}+\frac{\partial v}{\partial x}+\frac{\partial w}{\partial x}\frac{\partial w}{R\partial\theta}\right)+D_{66}\left(\frac{\partial\psi_x}{R\partial\theta}+\frac{\partial\psi_\theta}{\partial x}\right)+F_{66}\left(\frac{-4}{3h^2}\left(\frac{\partial\psi_\theta}{\partial x}+\frac{\partial\psi_x}{R\partial\theta}+2\frac{\partial^2 w}{R\partial x\partial\theta}\right)\right)\right)$$
$$+\frac{\partial}{R\partial\theta}\left(\begin{array}{l}B_{12}\left(\frac{\partial u}{\partial x}+\frac{1}{2}\left(\frac{\partial w}{\partial x}\right)^2\right)+B_{22}\left(\frac{\partial v}{R\partial\theta}+\frac{w}{R}+\frac{1}{2}\left(\frac{\partial w}{R\partial\theta}\right)^2\right)+D_{12}\left(\frac{\partial\psi_x}{\partial x}\right)+D_{22}\left(\frac{\partial\psi_\theta}{R\partial\theta}\right)\\+F_{12}\left(\frac{-4}{3h^2}\left(\frac{\partial\psi_x}{\partial x}+\frac{\partial^2 w}{\partial x^2}\right)\right)+F_{22}\left(\frac{-4}{3h^2}\left(\frac{\partial\psi_\theta}{R\partial\theta}+\frac{\partial^2 w}{R^2\partial\theta^2}\right)\right)\end{array}\right)$$
$$-A_{55}\left(\frac{\partial w}{R\partial\theta}+\psi_\theta\right)-D_{55}\left(\frac{-4}{h^2}\left(\psi_\theta+\frac{\partial w}{R\partial\theta}\right)\right)+\frac{4}{h^2}\left(D_{55}\left(\frac{\partial w}{R\partial\theta}+\psi_\theta\right)+F_{55}\left(\frac{-4}{h^2}\left(\psi_\theta+\frac{\partial w}{R\partial\theta}\right)\right)\right)$$

$$
\begin{aligned}
&-\frac{4}{3h^2}\left(\begin{array}{l}
\dfrac{\partial}{\partial x}\left(\begin{array}{l}
E_{66}\left(\dfrac{\partial u}{R\partial\theta}+\dfrac{\partial v}{\partial x}+\dfrac{\partial w}{\partial x}\dfrac{\partial w}{R\partial\theta}\right)+F_{66}\left(\dfrac{\partial \psi_x}{R\partial\theta}+\dfrac{\partial \psi_\theta}{\partial x}\right)\\
+H_{66}\left(\dfrac{-4}{3h^2}\left(\dfrac{\partial \psi_\theta}{\partial x}+\dfrac{\partial \psi_x}{R\partial\theta}+2\dfrac{\partial^2 w}{R\partial x\partial\theta}\right)\right)
\end{array}\right)\\
+\dfrac{\partial}{R\partial\theta}\left(\begin{array}{l}
E_{12}\left(\dfrac{\partial u}{\partial x}+\dfrac{1}{2}\left(\dfrac{\partial w}{\partial x}\right)^2\right)+E_{22}\left(\dfrac{\partial v}{R\partial\theta}+\dfrac{w}{R}+\dfrac{1}{2}\left(\dfrac{\partial w}{R\partial\theta}\right)^2\right)\\
+F_{12}\left(\dfrac{\partial \psi_x}{\partial x}\right)+F_{22}\left(\dfrac{\partial \psi_\theta}{R\partial\theta}\right)+H_{12}\left(\dfrac{-4}{3h^2}\left(\dfrac{\partial \psi_x}{\partial x}+\dfrac{\partial^2 w}{\partial x^2}\right)\right)\\
+H_{22}\left(\dfrac{-4}{3h^2}\left(\dfrac{\partial \psi_\theta}{R\partial\theta}+\dfrac{\partial^2 w}{R^2\partial\theta^2}\right)\right)
\end{array}\right)
\end{array}\right)\\
&=J_1\frac{\partial^2 v}{\partial t^2}+K_2\frac{\partial^2 \psi_\theta}{\partial t^2}-\frac{4}{3h^2}J_4\frac{\partial^3 w}{R\partial t^2\partial\theta}.
\end{aligned}
\tag{59}
$$

3. GDQM

There is a lot of numerical method to solve the initial-and/or boundary value problems which occur in engineering domain. Some of the common numerical methods are finite element method (FEM), Galerkin method, finite difference method (FDM), DQM and etc. FEM and FDM for higher-order modes require to a great number of grid points. Therefore these solution methods for all these points need to more CPU time, while the DQM has several benefits that are listed as below (Kolahchi *et al*. 2015b, Kolahchi and Moniribidgoli 2016):

1. DQM is a powerful method which can be used to solve numerical problems in the analysis of structural and dynamical systems.
2. The accuracy and convergence of the DQM is higher than FEM.
3. DQM is an accurate method for solution of nonlinear differential equations in approximation of the derivatives.
4. This method can easily and exactly satisfy a variety of boundary conditions and require much less formulation and programming effort.
5. Recently, DQM has been extended to handle irregular shaped.

Due to the above striking merits of the DQM, in recent years the method has become increasingly popular in the numerical solution of problems in engineering and physical science. In this method, the differential equations are changed into a first order algebraic equation by employing appropriate weighting coefficients. Because weighting coefficients do not relate to any special problem and only depend on the grid spacing. In other words, the partial derivatives of a function (say w here) are approximated with respect to specific variables (say x and θ), at a discontinuous point in a defined domain as a set of linear weighting coefficients and the amount represented by the function itself at that point and other points throughout the domain. The approximation of the n^{th} and m^{th} derivatives function with respect to x and y, respectively may be expressed in general form as (Abdollahian *et al*. 2013)

$$
\begin{aligned}
f_x^{(n)}(x_i,\theta_j) &= \sum_{k=1}^{N_x} A^{(n)}{}_{ik} f(x_k,\theta_j),\\
f_\theta^{(m)}(x_i,\theta_j) &= \sum_{l=1}^{N_\theta} B^{(m)}{}_{jl} f(x_i,\theta_l),\\
f_{x\theta}^{(n+m)}(x_i,\theta_j) &= \sum_{k=1}^{N_x}\sum_{l=1}^{N_\theta} A^{(n)}{}_{ik} B^{(m)}{}_{jl} f(x_k,\theta_l),
\end{aligned}
\tag{60}
$$

where N_x and N_θ, denotes the number of points in x and θ directions, $f(x, \theta)$ is the function and A_{ij}, B_{jl} are the weighting coefficients defined as

$$
\begin{aligned}
A^{(1)}{}_{ij} &= \frac{M(x_i)}{(x_i - x_j)M(x_i)},\\
B^{(1)}{}_{ij} &= \frac{P(\theta_i)}{(\theta_i - \theta_j)M(\theta_i)},
\end{aligned}
\tag{61}
$$

where M and P are Lagrangian operators defined as

$$
\begin{aligned}
M(x_i) &= \prod_{j=1}^{N_x}(x_i - x_j) \quad i \neq j,\\
P(\theta_i) &= \prod_{j=1}^{N_\theta}(\theta_i - \theta_j) \quad i \neq j.
\end{aligned}
\tag{62}
$$

The weighting coefficients for the second, third and fourth derivatives are determined via matrix multiplication

$$
\begin{aligned}
A^{(2)}{}_{ij} &= \sum_{k=1}^{N_x} A^{(1)}{}_{ik} A^{(1)}{}_{kj}, \quad A^{(3)}{}_{ij} = \sum_{k=1}^{N_x} A^{(2)}{}_{ik} A^{(1)}{}_{kj}, \quad A^{(4)}{}_{ij} = \sum_{k=1}^{N_x} A^{(3)}{}_{ik} A^{(1)}{}_{kj}, \quad i, j = 1,2,..., N_x,\\
B^{(2)}{}_{ij} &= \sum_{k=1}^{N_\theta} B^{(1)}{}_{ik} B^{(1)}{}_{kj}, \quad B^{(3)}{}_{ij} = \sum_{k=1}^{N_\theta} B^{(2)}{}_{ik} B^{(1)}{}_{kj}, \quad B^{(4)}{}_{ij} = \sum_{k=1}^{N_\theta} B^{(3)}{}_{ik} B^{(1)}{}_{kj}, \quad i, j = 1,2,..., N_\theta.
\end{aligned}
\tag{63}
$$

There are many typical grids such as equally space, Chebyshev, Legendre and Chebyshev-Gauss-Lobatto (Lobatto in short) grid points which are commonly used in the literature. For most cases, the original Lobatto grid is the best choice among the four traditional non-uniform grids. The stretched Lobatto grid with proper choice of stretching parameter can improve the accuracy of numerical solution (Shu *et al*. 2001). However, the distribution of grid points in domain is calculated by Chebyshev-Gauss-Lobatto polynomials as follows

$$
\begin{aligned}
x_i &= \frac{L}{2}\left[1 - \cos\left(\frac{\pi(i-1)}{(N_x - 1)}\right)\right],\\
\theta_j &= \frac{2\pi}{2}\left[1 - \cos\left(\frac{\pi(j-1)}{(N_\theta - 1)}\right)\right].
\end{aligned}
\tag{64}
$$

The solution of the motion equations can be assumed as follows:

$$u(x,\theta,t) = u_0(x,\theta)e^{\omega\tau}, \tag{65}$$

$$v(x,\theta,t) = v_0(x,\theta)e^{\omega\tau}, \tag{66}$$

$$w(x,\theta,t) = w_0(x,\theta)e^{\omega\tau}, \tag{67}$$

$$\psi_x(x,\theta,t) = \psi_{x0}(x,\theta)e^{\omega\tau}, \tag{68}$$

$$\psi_\theta(x,\theta,t) = \psi_{\theta0}(x,\theta)e^{\omega\tau}, \tag{69}$$

where $\omega = \lambda h\sqrt{\frac{\rho_f}{E}}$ and $\tau = \frac{t}{h}\sqrt{\frac{E}{\rho_f}}$ are the dimensionless natural frequency and dimensionless time. Substituting Eqs. (60) and (65)-(69) into the governing equations turns it into a set of algebraic equations expressed as

$$\begin{aligned}
&\delta u: A_{11}\left(\sum_{k=1}^{N_x} A^{(2)}{}_{ik}\,u(x_k,\theta_j) + \sum_{k=1}^{N_x} A^{(1)}{}_{ik}\,w(x_k,\theta_m)\sum_{k=1}^{N_x} A^{(2)}{}_{mk}\,w(x_k,\theta_j)\right) + \frac{A_{12}}{R^2}\left(R\sum_{k=1}^{N_x}\sum_{l=1}^{N_\theta} A^{(1)}{}_{ik}B^{(1)}{}_{jl}v(x_k,\theta_l)\right.\\
&\left. + R\sum_{k=1}^{N_x} A^{(1)}{}_{ik}\,w(x_k,\theta_j) + \sum_{l=1}^{N_\theta} B^{(1)}{}_{il}\,w(x_l,\theta_m)\sum_{k=1}^{N_x}\sum_{l=1}^{N_\theta} A^{(1)}{}_{mk}B^{(1)}{}_{jl}w(x_k,\theta_l)\right) + B_{11}\sum_{k=1}^{N_x} A^{(2)}{}_{ik}\,\psi_x(x_k,\theta_j) +\\
&\frac{B_{12}}{R}\sum_{k=1}^{N_x}\sum_{l=1}^{N_\theta} A^{(1)}{}_{ik}B^{(1)}{}_{jl}\,\psi_\theta(x_k,\theta_l) - \frac{4E_{11}}{3h^2}\left(\sum_{k=1}^{N_x} A^{(2)}{}_{ik}\psi_x(x_k,\theta_j) + \sum_{k=1}^{N_x} A^{(3)}{}_{ik}\,w(x_k,\theta_j)\right) - \frac{4E_{11}}{3R^2h^2}\\
&\left(R\sum_{k=1}^{N_x}\sum_{l=1}^{N_\theta} A^{(1)}{}_{ik}B^{(1)}{}_{jl}\psi_\theta(x_k,\theta_l) + \sum_{k=1}^{N_x}\sum_{l=1}^{N_\theta} A^{(1)}{}_{ik}B^{(2)}{}_{jl}w(x_k,\theta_l)\right) + \frac{A_{66}}{R^2}\left(\sum_{l=1}^{N_\theta} B^{(2)}{}_{il}u(x_l,\theta_j)\right.\\
&\left. + R\sum_{k=1}^{N_x}\sum_{l=1}^{N_\theta} A^{(1)}{}_{ik}B^{(1)}{}_{jl}v(x_k,\theta_l) + \sum_{l=1}^{N_\theta} B^{(1)}{}_{il}\,w(x_l,\theta_m)\sum_{k=1}^{N_x}\sum_{l=1}^{N_\theta} A^{(1)}{}_{mk}B^{(1)}{}_{jl}w(x_k,\theta_l)\right.\\
&\left. + \sum_{k=1}^{N_x} A^{(1)}{}_{ik}\,w(x_k,y_m)\sum_{l=1}^{N_\theta} B^{(2)}{}_{ml}w(x_l,\theta_j)\right) + \frac{B_{66}}{R^2}\left(\sum_{l=1}^{N_\theta} B^{(2)}{}_{il}\psi_x(x_l,\theta_j) + R\sum_{k=1}^{N_x}\sum_{l=1}^{N_\theta} A^{(1)}{}_{ik}B^{(1)}{}_{jl}\,\psi_\theta(x_k,\theta_l)\right)\\
&- \frac{4E_{66}}{3R^2h^2}\left(R\sum_{k=1}^{N_x}\sum_{l=1}^{N_\theta} A^{(1)}{}_{ik}B^{(1)}{}_{jl}\,\psi_\theta(x_k,\theta_l) + \sum_{l=1}^{N_\theta} B^{(2)}{}_{il}\psi_x(x_l,\theta_j) + 2\sum_{k=1}^{N_x}\sum_{l=1}^{N_\theta} A^{(1)}{}_{ik}B^{(2)}{}_{jl}\,w(x_k,\theta_l)\right)\\
&= \omega^2\left(I_0u(x_i,\theta_j) + J_1\psi_x(x_i,\theta_j) - \frac{4I_3}{h^2}\sum_{k=1}^{N_x} A^{(1)}{}_{ik}\,w(x_k,\theta_j)\right),
\end{aligned} \tag{70}$$

$$\begin{aligned}
&\delta v: \frac{A_{12}}{R}\left(\sum_{k=1}^{N_x}\sum_{l=1}^{N_\theta} A^{(1)}{}_{ik}B^{(1)}{}_{jl}u(x_k,\theta_l) + \sum_{k=1}^{N_x} A^{(1)}{}_{ik}\,w(x_k,\theta_m)\sum_{k=1}^{N_x}\sum_{l=1}^{N_\theta} A^{(1)}{}_{mk}B^{(1)}{}_{jl}w(x_k,\theta_l)\right) + \frac{A_{22}}{R^3}\left(R\sum_{l=1}^{N_\theta} B^{(2)}{}_{il}v(x_l,\theta_j)\right.\\
&\left. + R\sum_{l=1}^{N_\theta} B^{(1)}{}_{il}w(x_l,\theta_j) + \sum_{l=1}^{N_\theta} B^{(1)}{}_{il}\,w(x_l,\theta_m)\sum_{l=1}^{N_\theta} B^{(2)}{}_{ml}w(x_l,\theta_j)\right) + \frac{B_{22}}{R^2}\sum_{l=1}^{N_\theta} B^{(2)}{}_{il}\psi_\theta(x_l,\theta_j) +\\
&\frac{B_{12}}{R}\sum_{k=1}^{N_x}\sum_{l=1}^{N_\theta} A^{(1)}{}_{ik}B^{(1)}{}_{jl}\,\psi_x(x_k,\theta_l) - \frac{4E_{22}}{3R^3h^2}\left(R\sum_{l=1}^{N_\theta} B^{(2)}{}_{il}\psi_\theta(x_l,\theta_j) + \sum_{l=1}^{N_\theta} B^{(3)}{}_{il}w(x_l,\theta_j)\right) - \frac{4E_{12}}{3Rh^2}
\end{aligned}$$

$$\left(\sum_{k=1}^{N_x}\sum_{l=1}^{N_\theta}A^{(1)}{}_{ik}B^{(1)}{}_{jl}\psi_x(x_k,\theta_l)+\sum_{k=1}^{N_x}\sum_{l=1}^{N_\theta}A^{(2)}{}_{ik}B^{(1)}{}_{jl}w(x_k,\theta_l)\right)+\frac{A_{66}}{R}\left(R\sum_{k=1}^{N_x}A^{(2)}{}_{ik}v(x_k,\theta_j)+\sum_{k=1}^{N_x}\sum_{l=1}^{N_\theta}A^{(1)}{}_{ik}B^{(1)}{}_{jl}u(x_k,\theta_l)\right.$$
$$\left.+\sum_{l=1}^{N_\theta}B^{(1)}{}_{il}w(x_l,\theta_m)\sum_{k=1}^{N_x}A^{(2)}{}_{mk}w(x_k,\theta_j)+\sum_{k=1}^{N_x}A^{(1)}{}_{ik}w(x_k,\theta_m)\sum_{k=1}^{N_x}\sum_{l=1}^{N_\theta}A^{(1)}{}_{mk}B^{(1)}{}_{jl}w(x_k,\theta_l)\right)$$
$$+\frac{B_{66}}{R}\left(R\sum_{k=1}^{N_x}A^{(2)}{}_{ik}\psi_\theta(x_l,\theta_j)+R\sum_{k=1}^{N_x}\sum_{l=1}^{N_\theta}A^{(1)}{}_{ik}B^{(1)}{}_{jl}\psi_x(x_k,\theta_l)\right) \tag{71}$$
$$-\frac{4E_{66}}{3Rh^2}\left(R\sum_{k=1}^{N_x}\sum_{l=1}^{N_\theta}A^{(1)}{}_{ik}B^{(1)}{}_{jl}\psi_x(x_k,\theta_l)+R\sum_{k=1}^{N_x}A^{(2)}{}_{ik}\psi_\theta(x_l,\theta_j)+2\sum_{k=1}^{N_x}\sum_{l=1}^{N_\theta}A^{(2)}{}_{ik}B^{(1)}{}_{jl}w(x_k,\theta_l)\right)$$
$$=\omega^2\left(I_0v(x_i,\theta_j)+J_1\psi_\theta(x_i,\theta_j)-\frac{4I_3}{Rh^2}\sum_{l=1}^{N_\theta}B^{(1)}{}_{il}w(x_l,\theta_j)\right),$$

$$\delta w:\left(A_{55}-\frac{8D_{44}}{h^2}+\frac{16F_{44}}{h^4}\right)\left(\sum_{k=1}^{N_x}A^{(1)}{}_{ik}\psi_x(x_k,\theta_j)+\sum_{k=1}^{N_x}A^{(2)}{}_{ik}w(x_k,\theta_j)\right)+\left(\frac{A_{55}}{R^2}-\frac{4D_{55}}{R^2h^2}+\frac{D_{55}}{R^2}-\frac{4F_{55}}{Rh^2}\right)$$
$$\left(R\sum_{l=1}^{N_\theta}B^{(1)}{}_{il}\psi_\theta(x_l,\theta_j)+\sum_{l=1}^{N_\theta}B^{(2)}{}_{il}w(x_l,\theta_j)\right)+\left(N_{xx}^T+N_{xx}^M\right)\sum_{k=1}^{N_x}A^{(2)}{}_{ik}w(x_k,y_j)+\frac{\left(N_{\theta\theta}^T+N_{\theta\theta}^M\right)}{R^2}\sum_{l=1}^{N_\theta}B^{(2)}{}_{il}w(x_l,\theta_j)$$
$$+\frac{4E_{11}}{3h^2}\left(\sum_{k=1}^{N_x}A^{(3)}{}_{ik}u(x_k,\theta_j)+\sum_{k=1}^{N_x}A^{(2)}{}_{ik}w(x_k,\theta_m)\sum_{k=1}^{N_x}A^{(2)}{}_{mk}w(x_k,\theta_j)+\sum_{k=1}^{N_x}A^{(1)}{}_{ik}w(x_k,\theta_m)\sum_{k=1}^{N_x}A^{(3)}{}_{mk}w(x_k,\theta_j)\right)$$
$$+\frac{4E_{12}}{3h^2R^2}\left(R\sum_{k=1}^{N_x}\sum_{l=1}^{N_\theta}A^{(2)}{}_{ik}B^{(1)}{}_{jl}v(x_k,\theta_l)+R\sum_{k=1}^{N_x}A^{(2)}{}_{ik}w(x_k,\theta_j)+\sum_{l=1}^{N_\theta}B^{(1)}{}_{il}w(x_l,\theta_m)\sum_{k=1}^{N_x}\sum_{l=1}^{N_\theta}A^{(1)}{}_{mk}B^{(1)}{}_{jl}w(x_k,\theta_l)\right.$$
$$\left.+\sum_{k=1}^{N_x}\sum_{l=1}^{N_\theta}A^{(1)}{}_{il}B^{(1)}{}_{lk}w(x_k,\theta_m)\sum_{k=1}^{N_x}\sum_{l=1}^{N_\theta}A^{(1)}{}_{mk}B^{(1)}{}_{jl}w(x_k,\theta_l)\right)+\frac{4F_{11}}{3h^2}\left(\sum_{k=1}^{N_x}A^{(3)}{}_{ik}\psi_x(x_k,\theta_j)\right)+\frac{4F_{12}}{3Rh^2}\left(\sum_{k=1}^{N_x}\sum_{l=1}^{N_\theta}A^{(2)}{}_{ik}B^{(1)}{}_{jl}\psi_\theta(x_k,\theta_l)\right)$$
$$-\frac{16H_{11}}{9h^4}\left(\sum_{k=1}^{N_x}A^{(3)}{}_{ik}\psi_x(x_k,\theta_j)+\sum_{k=1}^{N_x}A^{(4)}{}_{ik}w(x_k,\theta_j)\right)-\frac{16H_{12}}{9h^4R^2}\left(R\sum_{k=1}^{N_x}\sum_{l=1}^{N_\theta}A^{(2)}{}_{ik}B^{(1)}{}_{jl}\psi_\theta(x_k,\theta_l)+\sum_{k=1}^{N_x}\sum_{l=1}^{N_\theta}A^{(2)}{}_{ik}B^{(2)}{}_{jl}\psi_\theta(x_k,\theta_l)\right)$$
$$+\frac{8E_{66}}{3h^2R^2}\left(\sum_{k=1}^{N_x}\sum_{l=1}^{N_\theta}A^{(1)}{}_{ik}B^{(2)}{}_{jl}u(x_k,\theta_l)+R\sum_{k=1}^{N_x}\sum_{l=1}^{N_\theta}A^{(2)}{}_{ik}B^{(1)}{}_{jl}v(x_k,\theta_l)+\sum_{k=1}^{N_x}\sum_{l=1}^{N_\theta}A^{(2)}{}_{ik}B^{(1)}{}_{ml}u(x_k,\theta_l)\sum_{l=1}^{N_\theta}B^{(1)}{}_{ml}w(x_l,\theta_j)\right.$$
$$\left.+\sum_{k=1}^{N_x}\sum_{l=1}^{N_\theta}A^{(1)}{}_{ik}B^{(2)}{}_{ml}u(x_k,\theta_l)\sum_{l=1}^{N_x}A^{(1)}{}_{ml}w(x_l,\theta_j)\right)+\frac{8F_{66}}{3h^2R^2}\left(\sum_{k=1}^{N_x}\sum_{l=1}^{N_\theta}A^{(1)}{}_{ik}B^{(2)}{}_{jl}\psi_x(x_k,\theta_l)+R\sum_{k=1}^{N_x}\sum_{l=1}^{N_\theta}A^{(2)}{}_{ik}B^{(1)}{}_{jl}\psi_\theta(x_k,\theta_l)\right)$$
$$-\frac{32H_{66}}{9h^4R^2}\left(R\sum_{k=1}^{N_x}\sum_{l=1}^{N_\theta}A^{(2)}{}_{ik}B^{(1)}{}_{jl}\psi_\theta(x_k,\theta_l)+\sum_{k=1}^{N_x}\sum_{l=1}^{N_\theta}A^{(1)}{}_{ik}B^{(2)}{}_{jl}\psi_x(x_k,\theta_l)+2\sum_{k=1}^{N_x}\sum_{l=1}^{N_\theta}A^{(2)}{}_{ik}B^{(2)}{}_{jl}w(x_k,\theta_l)\right)$$
$$+\frac{4E_{22}}{3h^2R^4}\left(R\sum_{k=1}^{N_\theta}B^{(3)}{}_{ij}v(x_j,\theta_j)+R\sum_{k=1}^{N_\theta}B^{(2)}{}_{ij}w(x_j,\theta_j)+\sum_{k=1}^{N_\theta}B^{(3)}{}_{ik}w(x_k,\theta_m)\sum_{k=1}^{N_\theta}B^{(1)}{}_{ml}w(x_l,\theta_j)+\sum_{k=1}^{N_\theta}B^{(2)}{}_{ik}w(x_k,\theta_m)\sum_{k=1}^{N_\theta}B^{(2)}{}_{ml}w(x_l,\theta_j)\right)$$
$$+\frac{4E_{12}}{3h^2R^2}\left(\sum_{k=1}^{N_x}\sum_{l=1}^{N_\theta}A^{(1)}{}_{ik}B^{(2)}{}_{jl}u(x_k,\theta_l)+\sum_{k=1}^{N_x}A^{(1)}{}_{ik}w(x_k,\theta_m)\sum_{k=1}^{N_x}\sum_{l=1}^{N_\theta}A^{(1)}{}_{mk}B^{(2)}{}_{jl}w(x_k,\theta_l)\right.$$
$$\left.+\sum_{k=1}^{N_x}A^{(2)}{}_{ik}w(x_k,\theta_m)\sum_{k=1}^{N_x}\sum_{l=1}^{N_\theta}A^{(1)}{}_{mk}B^{(1)}{}_{jl}w(x_k,\theta_l)\right)+\frac{4F_{22}}{3R^3h^2}\left(\sum_{k=1}^{N_\theta}B^{(3)}{}_{ij}\psi_\theta(x_j,\theta_j)\right)+\frac{4F_{12}}{3R^2h^2}\left(\sum_{k=1}^{N_x}\sum_{l=1}^{N_\theta}A^{(1)}{}_{ik}B^{(2)}{}_{jl}\psi_x(x_k,\theta_l)\right)$$
$$-\frac{16H_{22}}{9h^4R^4}\left(R\sum_{k=1}^{N_\theta}B^{(3)}{}_{ij}\psi_\theta(x_j,\theta_j)+\sum_{k=1}^{N_\theta}B^{(4)}{}_{ij}w(x_j,\theta_j)\right)-\frac{16H_{12}}{9h^4R^2}\left(\sum_{k=1}^{N_x}\sum_{l=1}^{N_\theta}A^{(1)}{}_{ik}B^{(2)}{}_{jl}\psi_x(x_k,\theta_l)+\sum_{k=1}^{N_x}\sum_{l=1}^{N_\theta}A^{(2)}{}_{ik}B^{(2)}{}_{jl}w(x_k,\theta_l)\right)$$
$$-\frac{A_{12}}{R}\left(\sum_{k=1}^{N_x}A^{(1)}{}_{ik}u(x_k,\theta_j)+0.5\sum_{k=1}^{N_x}A^{(1)}{}_{ik}w(x_k,\theta_m)\sum_{k=1}^{N_x}A^{(1)}{}_{ml}w(x_l,\theta_j)\right)-\frac{A_{22}}{R^3}\left(R\sum_{l=1}^{N_\theta}B^{(1)}{}_{il}w(x_l,\theta_j)+Rw(x_i,\theta_j)+\right.$$
$$\left.0.5\sum_{k=1}^{N_\theta}B^{(1)}{}_{ik}w(x_k,\theta_j)\sum_{k=1}^{N_\theta}B^{(1)}{}_{ik}w(x_k,\theta_j)\right)-\frac{B_{12}}{R}\left(\sum_{k=1}^{N_x}A^{(1)}{}_{ik}\psi_x(x_k,\theta_j)\right)-\frac{B_{22}}{R^2}\left(\sum_{k=1}^{N_\theta}B^{(1)}{}_{ij}\psi_\theta(x_j,\theta_j)\right)$$
$$+\frac{4E_{12}}{3h^2}\left(\sum_{k=1}^{N_x}A^{(1)}{}_{ik}\psi_x(x_k,\theta_j)+\sum_{k=1}^{N_x}A^{(2)}{}_{ik}w(x_k,\theta_j)\right)+\frac{4E_{22}}{3h^2R^2}\left(R\sum_{k=1}^{N_\theta}B^{(1)}{}_{ij}\psi_\theta(x_j,\theta_j)+\sum_{k=1}^{N_\theta}B^{(2)}{}_{ij}w(x_j,\theta_j)\right)$$

$$
\begin{aligned}
&-\frac{2h_f}{R}\left(\mu\left(\dot{w}(x_i,\theta_j)+v_x\sum_{k=1}^{N_x}A^{(1)}{}_{ik}\,w(x_k,y_j)\right)\right)-\rho_f h_f\left(\ddot{w}(x_i,\theta_j)+2v_x\sum_{k=1}^{N_x}A^{(1)}{}_{ik}\,\dot{w}(x_k,\theta_j)+v_x^2\sum_{k=1}^{N_x}A^{(2)}{}_{ik}\,w(x_k,\theta_j)\right)\\
&+\frac{h_f}{R^2}\left(\mu\left(\sum_{l=1}^{N_\theta}B^{(2)}{}_{il}\dot{w}(x_l,\theta_j)+v_x\sum_{k=1}^{N_x}\sum_{l=1}^{N_\theta}A^{(1)}{}_{ik}B^{(2)}{}_{jl}u(x_k,\theta_l)\right)\right)+h_f\left(\mu\left(\sum_{k=1}^{N_x}A^{(2)}{}_{ik}\,\dot{w}(x_k,y_j)+v_x\sum_{k=1}^{N_x}A^{(3)}{}_{ik}\,w(x_k,y_j)\right)\right)\\
&+K_w\,w(x_i,\theta_j)-K_{g\xi}\left(\cos^2\theta\sum_{k=1}^{N_x}A^{(2)}{}_{ik}\,w(x_k,y_j)+\frac{2\cos\theta\sin\theta}{R}\sum_{k=1}^{N_x}\sum_{l=1}^{N_\theta}A^{(1)}{}_{ik}B^{(1)}{}_{jl}u(x_k,\theta_l)+\frac{\sin^2\theta}{R^2}\sum_{l=1}^{N_\theta}B^{(2)}{}_{il}w(x_l,\theta_j)\right)\\
&-K_{g\eta}\left(\sin^2\theta\sum_{k=1}^{N_x}A^{(2)}{}_{ik}\,w(x_k,y_j)-\frac{2\sin\theta\cos\theta}{R}\sum_{k=1}^{N_x}\sum_{l=1}^{N_\theta}A^{(1)}{}_{ik}B^{(1)}{}_{jl}u(x_k,\theta_l)+\frac{\cos^2\theta}{R^2}\sum_{l=1}^{N_\theta}B^{(2)}{}_{il}w(x_l,\theta_j)\right)\\
&=\omega^2\left(I_0 w(x_i,\theta_j)-\left(\frac{4}{3h^2}\right)^2 I_6\left(\sum_{k=1}^{N_x}A^{(2)}{}_{ik}\,w(x_k,\theta_j)+\frac{1}{R^2}\sum_{l=1}^{N_\theta}B^{(2)}{}_{il}w(x_l,\theta_j)\right)+\frac{4}{3h^2}\left(I_3\sum_{k=1}^{N_x}A^{(1)}{}_{ik}\,u(x_k,\theta_j)+\right.\right.\\
&\left.\left.\frac{I_3}{R}\sum_{l=1}^{N_\theta}B^{(1)}{}_{il}v(x_l,\theta_j)+J_4\left(\sum_{k=1}^{N_x}A^{(1)}{}_{ik}\psi_x(x_k,\theta_j)+\frac{1}{R}\sum_{l=1}^{N_\theta}B^{(1)}{}_{il}\psi_\theta(x_l,\theta_j)\right)\right)\right),
\end{aligned}
\tag{72}
$$

$$
\begin{aligned}
&\delta\psi_x:\ B_{11}\left(\sum_{k=1}^{N_x}A^{(2)}{}_{ik}\,u(x_k,\theta_j)+\sum_{k=1}^{N_x}A^{(1)}{}_{ik}\,w(x_k,\theta_m)\sum_{k=1}^{N_x}A^{(2)}{}_{mk}\,w(x_k,\theta_j)\right)+\frac{B_{12}}{R^2}\left(R\sum_{k=1}^{N_x}\sum_{l=1}^{N_\theta}A^{(1)}{}_{ik}B^{(1)}{}_{jl}v(x_k,\theta_l)\right.\\
&\left.+R\sum_{l=1}^{N_\theta}B^{(1)}{}_{il}v(x_l,\theta_j)+\sum_{l=1}^{N_\theta}B^{(1)}{}_{il}\,w(x_l,\theta_m)\sum_{k=1}^{N_x}\sum_{l=1}^{N_\theta}A^{(1)}{}_{mk}B^{(1)}{}_{jl}w(x_k,\theta_l)\right)+D_{11}\sum_{k=1}^{N_x}A^{(2)}{}_{ik}\psi_x(x_k,\theta_j)\\
&+\frac{D_{12}}{R}\sum_{k=1}^{N_x}\sum_{l=1}^{N_\theta}A^{(1)}{}_{ik}B^{(1)}{}_{jl}\psi_\theta(x_k,\theta_l)-\frac{4F_{11}}{3h^2}\left(\sum_{k=1}^{N_x}A^{(2)}{}_{ik}\psi_x(x_k,\theta_j)+\sum_{k=1}^{N_x}A^{(3)}{}_{ik}\,w(x_k,\theta_j)\right)\\
&-\frac{4F_{12}}{3h^2R^2}\left(R\sum_{k=1}^{N_x}\sum_{l=1}^{N_\theta}A^{(1)}{}_{ik}B^{(1)}{}_{jl}\psi_\theta(x_k,\theta_l)+\sum_{l=1}^{N_\theta}B^{(3)}{}_{il}w(x_l,\theta_j)\right)+\frac{B_{66}}{R^2}\left(\sum_{l=1}^{N_\theta}B^{(2)}{}_{il}u(x_l,\theta_j)+\right.\\
&\left.R\sum_{k=1}^{N_x}\sum_{l=1}^{N_\theta}A^{(1)}{}_{ik}B^{(1)}{}_{jl}v(x_k,\theta_l)+\sum_{k=1}^{N_x}\sum_{l=1}^{N_\theta}A^{(1)}{}_{ik}B^{(1)}{}_{ml}w(x_k,\theta_l)\sum_{l=1}^{N_\theta}B^{(1)}{}_{ml}w(x_l,\theta_j)+\sum_{k=1}^{N_x}A^{(1)}{}_{ik}\,w(x_k,\theta_m)\sum_{l=1}^{N_\theta}B^{(2)}{}_{ml}w(x_l,\theta_j)\right)\\
&\frac{D_{66}}{R^2}\left(\sum_{l=1}^{N_\theta}B^{(2)}{}_{il}\,\psi_x(x_l,\theta_j)+R\sum_{k=1}^{N_x}\sum_{l=1}^{N_\theta}A^{(1)}{}_{ik}B^{(1)}{}_{jl}\psi_\theta(x_k,\theta_l)\right)-\frac{4F_{66}}{3h^2R^2}\left(R\sum_{k=1}^{N_x}\sum_{l=1}^{N_\theta}A^{(1)}{}_{ik}B^{(1)}{}_{jl}\psi_\theta(x_k,\theta_l)\right.\\
&\left.\sum_{l=1}^{N_\theta}B^{(2)}{}_{il}\,\psi_x(x_l,\theta_j)+2\sum_{k=1}^{N_x}\sum_{l=1}^{N_\theta}A^{(1)}{}_{ik}B^{(2)}{}_{jl}w(x_k,\theta_l)-\left(A_{44}-\frac{8D_{66}}{h^2}+\frac{4F_{44}}{h^2}\right)\left(\psi_x(x_i,\theta_j)+\sum_{k=1}^{N_x}A^{(1)}{}_{ik}\,w(x_k,\theta_j)\right)\right.\\
&-\frac{4E_{11}}{3h^2}\left(\sum_{k=1}^{N_x}A^{(2)}{}_{ik}\,u(x_k,\theta_j)+\sum_{k=1}^{N_x}A^{(1)}{}_{ik}\,w(x_k,\theta_m)\sum_{k=1}^{N_x}A^{(2)}{}_{mk}\,w(x_k,\theta_j)\right)-\frac{4E_{12}}{3h^2R^2}\left(R\sum_{k=1}^{N_x}\sum_{l=1}^{N_\theta}A^{(1)}{}_{ik}B^{(1)}{}_{jl}v(x_k,\theta_l)\right.\\
&\left.+R\sum_{l=1}^{N_\theta}B^{(1)}{}_{il}v(x_l,\theta_j)+\sum_{l=1}^{N_\theta}B^{(1)}{}_{il}\,w(x_l,\theta_m)\sum_{k=1}^{N_x}\sum_{l=1}^{N_\theta}A^{(1)}{}_{mk}B^{(1)}{}_{jl}w(x_k,\theta_l)\right)-\frac{4F_{11}}{3h^2}\left(\sum_{k=1}^{N_x}A^{(1)}{}_{ik}\psi_x(x_k,\theta_j)\right)\\
&-\frac{4F_{12}}{3h^2R}\left(\sum_{k=1}^{N_x}\sum_{l=1}^{N_\theta}A^{(1)}{}_{ik}B^{(1)}{}_{jl}\psi_\theta(x_k,\theta_l)\right)+\frac{16H_{11}}{9h^4}\left(\sum_{k=1}^{N_x}A^{(2)}{}_{ik}\psi_x(x_k,\theta_j)+\sum_{k=1}^{N_x}A^{(3)}{}_{ik}\,w(x_k,\theta_j)\right)\\
&+\frac{16H_{12}}{9h^4R^2}\left(\sum_{k=1}^{N_x}\sum_{l=1}^{N_\theta}A^{(1)}{}_{ik}B^{(1)}{}_{jl}\psi_\theta(x_k,\theta_l)+\sum_{k=1}^{N_x}\sum_{l=1}^{N_\theta}A^{(1)}{}_{ik}B^{(2)}{}_{jl}w(x_k,\theta_l)\right)-\frac{4E_{66}}{3h^2R^2}\left(\sum_{l=1}^{N_\theta}B^{(2)}{}_{il}\,u(x_l,\theta_j)\right.\\
&\left.+R\sum_{k=1}^{N_x}\sum_{l=1}^{N_\theta}A^{(1)}{}_{ik}B^{(1)}{}_{jl}v(x_k,\theta_l)+\sum_{k=1}^{N_x}\sum_{l=1}^{N_\theta}A^{(1)}{}_{ik}B^{(1)}{}_{ml}w(x_k,\theta_l)\sum_{l=1}^{N_\theta}B^{(1)}{}_{ml}w(x_l,\theta_j)+\sum_{k=1}^{N_x}A^{(1)}{}_{ik}\,w(x_k,\theta_m)\sum_{l=1}^{N_\theta}B^{(2)}{}_{ml}w(x_l,\theta_j)\right)\\
&-\frac{4F_{66}}{3h^2R^2}\left(\sum_{l=1}^{N_\theta}B^{(2)}{}_{il}\,\psi_x(x_l,\theta_j)+R\sum_{k=1}^{N_x}\sum_{l=1}^{N_\theta}A^{(1)}{}_{ik}B^{(1)}{}_{jl}\psi_\theta(x_k,\theta_l)\right)+\frac{16H_{66}}{9h^4R^2}\left(R\sum_{k=1}^{N_x}\sum_{l=1}^{N_\theta}A^{(1)}{}_{ik}B^{(1)}{}_{jl}\psi_\theta(x_k,\theta_l)\right.\\
&\left.\sum_{l=1}^{N_\theta}B^{(2)}{}_{il}\,\psi_x(x_l,\theta_j)+2\sum_{k=1}^{N_x}\sum_{l=1}^{N_\theta}A^{(1)}{}_{ik}B^{(2)}{}_{jl}w(x_k,\theta_l)\right)=\omega^2\left(K_2\psi_x(x_i,\theta_j)+J_1u(x_i,\theta_j)-\frac{4}{3h^2}J_4\sum_{k=1}^{N_x}A^{(1)}{}_{ik}\,w(x_k,\theta_j)\right),
\end{aligned}
\tag{73}
$$

$$\delta\psi_\theta : \frac{B_{66}}{R}\left(\sum_{k=1}^{N_x}\sum_{l=1}^{N_\theta} A^{(1)}{}_{ik}B^{(1)}{}_{jl}u(x_k,\theta_l) + R\sum_{k=1}^{N_x} A^{(2)}{}_{ik}v(x_k,\theta_j) + \sum_{k=1}^{N_x} A^{(2)}{}_{ik}w(x_k,\theta_m)\sum_{l=1}^{N_\theta} B^{(1)}{}_{ml}w(x_l,\theta_j)\right)$$
$$+\frac{D_{66}}{R}\left(\sum_{k=1}^{N_x}\sum_{l=1}^{N_\theta} A^{(1)}{}_{ik}B^{(1)}{}_{jl}\psi_x(x_k,\theta_l) + R\sum_{k=1}^{N_x} A^{(2)}{}_{ik}\psi_\theta(x_k,\theta_j)\right) - \frac{4F_{66}}{3h^2R}\left(R\sum_{k=1}^{N_x} A^{(2)}{}_{ik}\psi_\theta(x_k,\theta_j) +\right.$$
$$\left.\sum_{k=1}^{N_x}\sum_{l=1}^{N_\theta} A^{(1)}{}_{ik}B^{(1)}{}_{jl}\psi_x(x_k,\theta_l) + \sum_{k=1}^{N_x}\sum_{l=1}^{N_\theta} A^{(2)}{}_{ik}B^{(1)}{}_{jl}w(x_k,\theta_l)\right) + \frac{B_{12}}{R}\left(\sum_{k=1}^{N_x}\sum_{l=1}^{N_\theta} A^{(1)}{}_{ik}B^{(1)}{}_{jl}u(x_k,\theta_l)\right.$$
$$\left.+\sum_{k=1}^{N_x} A^{(1)}{}_{ik}w(x_k,\theta_m)\sum_{k=1}^{N_x}\sum_{l=1}^{N_\theta} A^{(1)}{}_{mk}B^{(1)}{}_{jl}w(x_k,\theta_l)\right) + \frac{B_{22}}{R^3}\left(R\sum_{l=1}^{N_\theta} B^{(2)}{}_{il}v(x_l,\theta_j) + R\sum_{l=1}^{N_\theta} B^{(1)}{}_{il}w(x_l,\theta_j)\right.$$
$$\left.+\sum_{l=1}^{N_\theta} B^{(1)}{}_{il}w(x_l,\theta_m)\sum_{k=1}^{N_x}\sum_{l=1}^{N_\theta} A^{(1)}{}_{mk}B^{(1)}{}_{jl}w(x_k,\theta_l)\right) + \frac{D_{12}}{R}\sum_{k=1}^{N_x}\sum_{l=1}^{N_\theta} A^{(1)}{}_{ik}B^{(1)}{}_{jl}\psi_x(x_k,\theta_l)$$
$$+\frac{D_{22}}{R^2}\sum_{l=1}^{N_\theta} B^{(2)}{}_{il}\psi_\theta(x_l,\theta_j) - \frac{4F_{12}}{3h^2R}\left(\sum_{k=1}^{N_x}\sum_{l=1}^{N_\theta} A^{(1)}{}_{ik}B^{(1)}{}_{jl}\psi_x(x_k,\theta_l) + \sum_{k=1}^{N_x}\sum_{l=1}^{N_\theta} A^{(1)}{}_{ik}B^{(2)}{}_{jl}w(x_k,\theta_l)\right)$$
$$-\frac{4F_{22}}{3h^2R^2}\left(R\sum_{l=1}^{N_\theta} B^{(2)}{}_{il}\psi_\theta(x_l,\theta_j) + \sum_{l=1}^{N_\theta} B^{(3)}{}_{il}\psi_\theta w(x_l,\theta_j)\right) - \left(\frac{A_{55}}{R} - \frac{8D_{55}}{h^2R} + \frac{4F_{55}}{h^2R}\right)$$
$$\left(R\psi_\theta(x_i,\theta_j) + \sum_{l=1}^{N_\theta} B^{(1)}{}_{il}w(x_l,\theta_j)\right) - \frac{4E_{66}}{3h^2R}\left(\sum_{k=1}^{N_x}\sum_{l=1}^{N_\theta} A^{(1)}{}_{ik}B^{(1)}{}_{jl}u(x_k,\theta_l) + R\sum_{k=1}^{N_x} A^{(2)}{}_{ik}\psi_\theta(x_k,\theta_j)\right. \tag{74}$$
$$\left.\sum_{k=1}^{N_x} A^{(1)}{}_{ik}w(x_k,\theta_m)\sum_{k=1}^{N_x}\sum_{l=1}^{N_\theta} A^{(1)}{}_{mk}B^{(1)}{}_{jl}w(x_k,\theta_l) + \sum_{k=1}^{N_\theta} B^{(1)}{}_{il}w(x_l,\theta_m)\sum_{k=1}^{N_x}\sum_{l=1}^{N_\theta} A^{(1)}{}_{mk}B^{(1)}{}_{jl}w(x_k,\theta_l)\right)$$
$$-\frac{4F_{66}}{3h^2R}\left(\sum_{k=1}^{N_x}\sum_{l=1}^{N_\theta} A^{(1)}{}_{ik}B^{(1)}{}_{jl}\psi_x(x_k,\theta_l) + \sum_{l=1}^{N_x} A^{(2)}{}_{ik}\psi_\theta(x_k,\theta_j)\right) + \frac{16H_{66}}{9h^4R^2}\left(R\sum_{k=1}^{N_x} A^{(2)}{}_{ik}\psi_\theta(x_k,\theta_j)\right.$$
$$\left.+\sum_{k=1}^{N_x}\sum_{l=1}^{N_\theta} A^{(1)}{}_{ik}B^{(1)}{}_{jl}\psi_x(x_k,\theta_l) + 2\sum_{l=1}^{N_\theta}\sum_{k=1}^{N_x} A^{(2)}{}_{ik}B^{(1)}{}_{jl}w(x_k,\theta_l)\right) - \frac{4E_{12}}{3h^2R}\left(\sum_{k=1}^{N_x}\sum_{l=1}^{N_\theta} A^{(1)}{}_{ik}B^{(1)}{}_{jl}u(x_k,\theta_l)\right.$$
$$\left.\sum_{k=1}^{N_x} A^{(1)}{}_{ik}w(x_k,\theta_m)\sum_{k=1}^{N_x}\sum_{l=1}^{N_\theta} A^{(1)}{}_{mk}B^{(1)}{}_{jl}w(x_k,\theta_l)\right) - \frac{4E_{22}}{3h^2R^3}\left(R\sum_{l=1}^{N_\theta} B^{(2)}{}_{il}v(x_l,\theta_j) + R\sum_{l=1}^{N_\theta} B^{(1)}{}_{il}w(x_l,\theta_j)\right.$$
$$\left.\sum_{k=1}^{N_\theta} B^{(2)}{}_{il}w(x_l,\theta_m)\sum_{k=1}^{N_\theta} B^{(2)}{}_{ml}w(x_l,\theta_m)\right) - \frac{4F_{12}}{3h^2R}\left(\sum_{k=1}^{N_x}\sum_{l=1}^{N_\theta} A^{(1)}{}_{ik}B^{(1)}{}_{jl}\psi_x(x_k,\theta_l)\right)$$
$$-\frac{4F_{22}}{3h^2R^2}\left(\sum_{l=1}^{N_\theta} B^{(2)}{}_{il}\psi_\theta(x_l,\theta_j)\right) + \frac{16H_{12}}{9h^4R}\left(\sum_{k=1}^{N_x}\sum_{l=1}^{N_\theta} A^{(1)}{}_{ik}B^{(1)}{}_{jl}\psi_x(x_k,\theta_l) + \sum_{k=1}^{N_x}\sum_{l=1}^{N_\theta} A^{(2)}{}_{ik}B^{(1)}{}_{jl}w(x_k,\theta_l)\right)$$
$$+\frac{16H_{22}}{9h^4R^3}\left(R\sum_{l=1}^{N_\theta} B^{(2)}{}_{il}\psi_\theta(x_l,\theta_j) + \sum_{l=1}^{N_\theta} B^{(3)}{}_{il}w(x_l,\theta_j)\right) = \omega^2\left(K_2\psi_\theta(x_i,\theta_j) + J_1v(x_i,\theta_j) - \frac{4}{3h^2}J_4\sum_{l=1}^{N_\theta} B^{(1)}{}_{il}w(x_l,\theta_j)\right).$$

Finally, the governing equations (i.e., Eqs. (70)- (74)) in matrix form can be expressed as

$$\left[[K_L + K_{NL}] + [C]\omega + [M]\omega^2\right][d] = [0], \tag{75}$$

where $[d]=[u\ v\ w\ \psi_x\ \psi_y]^T$; [*KL*] and [*KNL*] are respectively, linear and nonlinear stiffness matrixes; [*C*] is damp matrix and [*M*] is the mass matrix. For solving the Eq. (75) and reducing it to the standard form of eigenvalue problem, it is convenient to rewrite Eq. (75) as the following first order variable as

$$\left\{\dot{\mathrm{Z}}\right\} = \left[\mathrm{A}\right]\left\{\mathrm{Z}\right\}, \tag{76}$$

in which the state vector Z and state matrix $[A]$ are defined as

$$Z=\begin{Bmatrix} d_d \\ \dot{d}_d \end{Bmatrix} \text{ and } [A]=\begin{bmatrix} [0] & [I] \\ -\left[M^{-1}\left(K_L+K_{NL}\right)\right] & -\left[M^{-1}C\right] \end{bmatrix}, \tag{77}$$

where [0] and [I] are the zero and unitary matrices, respectively. However, the frequencies obtained from the solution of Eq. (77) are complex due to the damping existed in the presence of the viscous fluid flow. Hence, the results are containing two real and imaginary parts. The real part is corresponding to the system damping, and the imaginary part representing the system natural frequencies. This nonlinear equation can now be solved using a direct iterative process as follows:

- First, nonlinearity is ignored by taking K_{NL}=0 to solve the eigenvalue problem expressed in Eq. (77). This yields the linear eigenvalue and associated eigenvector. The eigenvector is then scaled up so that the maximum transverse displacement of the pipe is equal to the maximum eigenvector, i.e., the given vibration amplitude w_{max}.
- Using linear w, $[K_{NL}]$ could be evaluated. Eigenvalue problem is then solved by substituting $[K_{NL}]$ into Eq. (7). This would give the nonlinear eigenvalue and the new eigenvector.
- The new nonlinear eigenvector is scaled up again and the above procedure is repeated iteratively until the frequency values from the two subsequent iterations 'r' and 'r+1' satisfy the prescribed convergence criteria as

$$\frac{\left|\omega^{r+1}-\omega^{r}\right|}{\omega^{r}}<\varepsilon_0, \tag{78}$$

where ε_0 is a small value number and in the present analysis it is taken to be 0.1%

4. Numerical results and discussion

A computer program is prepared for the numerical solution of vibration and stability of FG pipe resting on orthotropic Pasternak foundation. Here, a mixture of zirconium oxide and titanium alloy, referred to as ZrO2/Ti-6Al-4V for the FGM pipe is selected. The FGM properties, P, can be expressed as nonlinear functions of environment temperature T as (Mirzavand and Eslami 2011)

$$P=P_0\left(P_{-1}T^{-1}+1+P_1T+P_2T^2+P_3T^3\right), \tag{79}$$

which $T=T_0+\Delta T$ and T_0=300K (room temperature); P_0, P_{-1}, P_1, P_2, P_3 are temperature dependent coefficients that are unique to the constituent materials. Typical values for Young's modulus E, Poison's ratio v, and the coefficient of thermal expansion α of zirconium oxide and titanium alloy are listed in Table1. The elastomeric medium is made of Poly dimethylsiloxane (PDMS) which the temperature-dependent material properties of which are assumed to be v_s=0.48 and E_s=(3.22−0.0034T)GPa in which $T=T_0+\Delta T$ and T_0=300K (room temperature) (Shen and Zhang, 2011). The FG pipes are considered with three kinds of boundary conditions: simply supported at both ends (SS) or clamped (CC), and one end simply supported and another clamped (SC) (Xing *et al*. 2013). In addition, the nanoparticle-fluid mixture is made of Al_2O_3-water suspension with variant volume fractions of particles (Ghorbanpour Arani *et al*. 2016).

Table 1 Temperature-dependent material coefficients for zirconium oxide and titanium alloy

Material properties	Material	P_0	P_{-1}	P_1	P_2	P_3
E (Pa)	Zirconium oxide	244.27e+9	0	-1.371e-3	1.214e-6	-3.681e-10
	Titanium alloy	122.56e+9	0	-4.586e-4	0	0
v	Zirconium oxide	0.28	0	0	0	0
	Titanium alloy	0.28	0	0	0	0
α (1/K)	Zirconium oxide	12.766e-6	0	-1.491e-3	1.006e-5	-6.778e-11
	Titanium alloy	7.5788e-6	0	6.638e-4	-3.147e6	0

Table 2 Accuracy of the GDQM for frequency of FG pipe

N_θ	N_x	SS	CC
7	7	0.7117	0.8272
	11	0.9945	1.1518
	15	1.1788	1.4124
	17	1.1788	1.4124
11	7	0.9551	1.2834
	11	1.1011	1.4136
	15	1.1855	1.4262
	17	1.1855	1.4262
15	7	0.9698	1.2942
	11	1.1855	1.4266
	15	1.1864	1.4273
	17	1.1864	1.4273
17	7	1.0704	1.3068
	11	1.1860	1.4270
	15	1.1864	1.4273
	17	1.1864	1.4273

4.1 Convergence of GDQM

The convergence and accuracy of the DQM in evaluating the excitation frequency of the FG pipe is shown in Table 2. The results are prepared for different values of the DQM grid points. Fast rate of convergence of the method are quite evident and it is found that fifteen DQ grid points can yield accurate results.

4.2 Validation

In the absence of similar publications in the literature covering the same scope of the problem, one can not directly validate the results found here. However, the present work could be partially validated based on a simplified analysis suggested by Yang and Shen (2003), Pradyumna and Bandyopadhyay (2008), Neves *et al*. (2013) and Fazzolari and Erasmo Carrera (2014). Hence, vibration of clamped supported classical cylindrical shells is investigated where the temperature

dependency of material, elastic medium and fluid are ignored. The geometrical parameters of the shell are assumed are L/h=10 and R/L=100. Furthermore, the shell made up of Si3 (ceramic) and SUS304 (metal) with E_c=322.2715 GPa, ν_c=0.24, ρ_c=2370 Kg/m^3, E_m=207.7877 GPa, ν_m=0.31 and ρ_m=8166 Kg/m^3. Table 3 illustrates the first four dimensionless frequency ($\Omega = \omega L^2\sqrt{\rho_m/D_m}$) with $D_m=E_m h^3/[12(1-\nu_m{}^2)]$ for different FG gradient index. As can be seen, the obtained results are the same as those expressed by Yang and Shen (2003), Pradyumna and Bandyopadhyay (2008), Neves *et al*. (2013) and Fazzolari and Erasmo Carrera (2014), indicating validation of our work.

Noted that the little difference between present work and other references is due to the type of applied theory and solution method. In the works of Yang and Shen (2003), Pradyumna and

Table 3 First four dimensionless frequency parameters of clamped FGM cylindrical shell for different FG index

Mode	Theory	g				
		0	0.2	2	10	∞
1	HSDT, Pradyumna and Bandyopadhyay (2008)	72.9613	60.0269	39.1457	33.3666	32.-274
	HSDT, Fazzolari and Carrera (2014)	75.2498	61.3403	41.1511	35.6545	33.2433
	HSDT, Yang and Shen (2003)	74.518	57.479	40.750	35.852	32.761
	HSDT, Neves *et al*. (2013)	74.2634	60.0061	40.5259	35.1663	32.6108
	HSDT, Neves *et al*. (2013)	74.5821	60.3431	40.8262	35.4229	32.8593
	RSDT, Present work	74.7832	60.9912	40.8812	35.5512	32.1434
2	HSDT, Pradyumna and Bandyopadhyay (2008)	138.5552	113.8806	74.2915	63.2869	60.5546
	HSDT, Fazzolari and Carrera (2014)	143.5110	116.9275	78.1359	67.5201	63.0894
	HSDT, Yang and Shen (2003)	144.663	111.717	78.817	69.075	63.314
	HSDT, Neves *et al*. (2013)	141.6779	114.3788	76.9725	66.6482	61.9329
	HSDT, Neves *et al*. (2013)	142.4281	115.2134	77.6639	67.1883	62.4886
	RSDT, Present work	143.2016	116.0127	78.0034	67.3936	63.0088
3	HSDT, Pradyumna and Bandyopadhyay (2008)	138.5552	114.0266	74.3868	63.3668	60.6302
	HSDT, Fazzolari and Carrera (2014)	143.6735	117.0744	78.2242	67.5946	63.1603
	HSDT, Yang and Shen (2003)	145.740	112.531	79.407	69.609	63.806
	HSDT, Neves *et al*. (2013)	141.8485	114.5495	77.0818	66.7332	62.0082
	HSDT, Neves *et al*. (2013)	142.6024	115.3665	77.7541	67.2689	62.5668
	RSDT, Present work	143.5908	116.6010	78.0582	67.4452	63.0245
4	HSDT, Pradyumna and Bandyopadhyay (2008)	195.5366	160.6235	104.7687	89.1970	85.1788
	HSDT, Fazzolari and Carrera (2014)	201.6888	164.2966	109.5277	94.4779	88.3744
	HSDT, Yang and Shen (2003)	206.992	159.855	112.457	98.386	90.370
	HSDT, Neves *et al*. (2013)	199.1566	160.7355	107.9484	93.3350	86.8160
	HSDT, Neves *et al*. (2013)	200.3158	162.0337	108.9677	94.0923	86.6341
	RSDT, Present work	201.2230	163.9014	109.1110	94.2046	87.9103

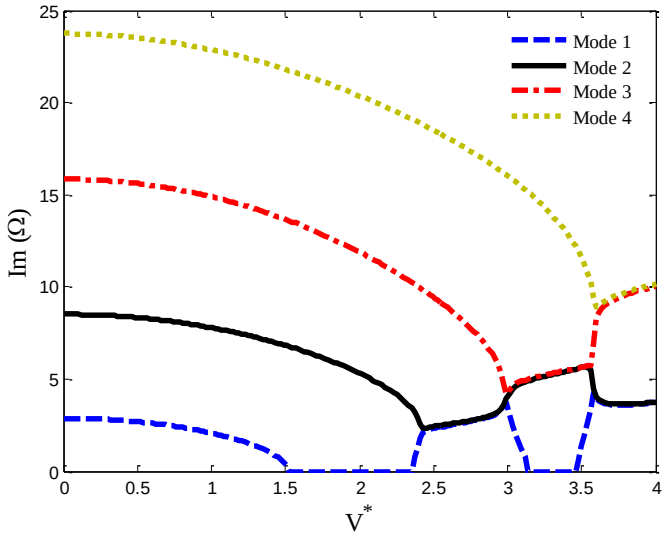

Fig. 2 Effects of mode numbers on the dimension frequency (Im(Ω)) versus dimension flow velocity

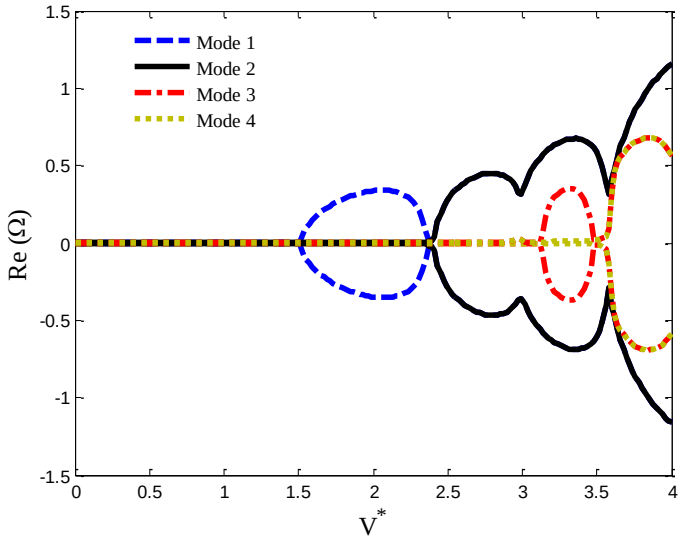

Fig. 3 Effects of mode numbers on the dimension frequency (Re(Ω)) versus dimension flow velocity

Bandyopadhyay (2008), Neves *et al*. (2013), Fazzolari and Erasmo Carrera (2014), the higher order shear deformation theory (HSDT) and semi-analytical approach, HSDT and finite element method, HSDT and radial basis functions, refined hierarchical kinematics (RHK) and Ritz method are used, respectively while in the present study, the RSDT in conjunction with GDQM is applied.

4.3 Effect of different parameters

Figs. 2 and 3 show the dimensionless frequency (Im(Ω)) and damping (Re(Ω)) of FG pipe

versus the dimensionless flow velocity ($V^* = \sqrt{\rho_f / C_{11}}\, v_x$) for the first four modes of vibration, respectively. Generally, the system is stable when the real part of the frequency remains zero and it is unstable when the real and imaginary parts of the frequency become positive and zero, respectively. It can be seen that the Im(Ω) generally decreases with increasing V^*. For zero frequency, FG pipe becomes unstable and the corresponding fluid velocity is called the critical flow velocity. As can be seen, the critical fluid velocity correspond to the first mode is reached at V^*=1.508. This physically impalas that the pipe losses its stability due to the divergence via a pitchfork bifurcation while the second, third and fourth modes are still stable. Thereafter, for the fluid velocity within the range 1.508<V^*<2.352, the Re(Ω) of the first mode is positive, which the system becomes unstable. Afterwards, the Im(Ω) of the first and second modes combines to each other in the region of 2.432<V^*<2.995. This physically implies a single coupled-mode between the first and the second modes occurs which is unstable with flutter instability. Also, this phenomenon may be observed in different modes for higher velocities. For example, a coupled-mode between the second and the third modes takes place in the range of 3.015≤V^*≤3.558. Meanwhile, it should be noted that the pipe becomes unstable at second, third and fourth modes when $V^* \cong 2.432$, $V^* \cong 2.995$ and $V^* \cong 3.638$ respectively.

Figs. 4 and 5 show the effect of gradient index on the dimensionless frequency (and damping of FG pipe versus dimensionless flow velocity, respectively. With increasing flow velocity, system stability decreases and became susceptible to buckling. It can be observed that, the Im(Ω) o and critical fluid velocity of system decrease with increasing gradient index. This decrease in frequency and critical fluid velocity with power law index is attributed to the fact that zirconium oxide has larger stiffness than that of titanium alloy. When the value of power-law index is zero, FGM pipe consists of only zirconium oxide. Thus, frequency and critical fluid velocity values are maximum when g is zero. With increase of g value, the more metal materials are included in the FGM pipe. It is worth mentioning that the results this figure, exhibiting increase of frequency and critical fluid velocity with lower value of g, i.e., for zirconium oxide, which is lighter than the

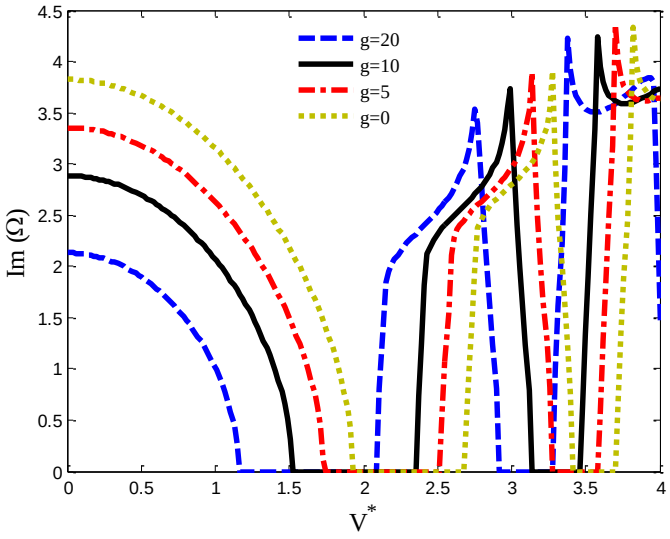

Fig. 4 Effects of gradient index on the dimension frequency (Im(Ω)) versus dimension flow velocity

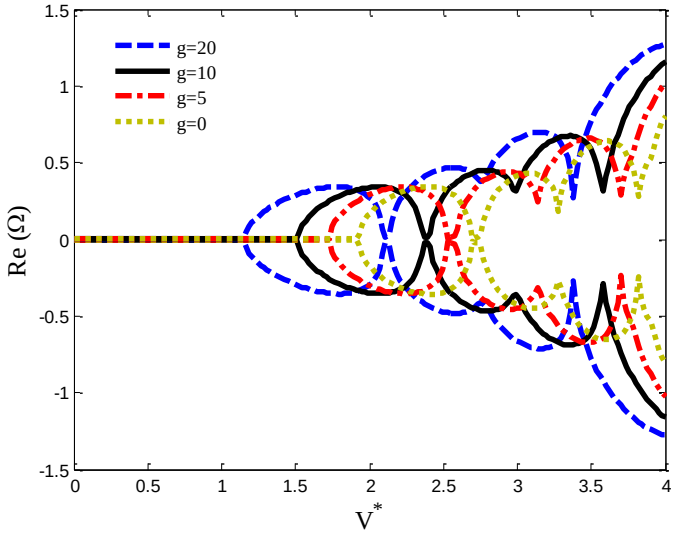

Fig. 5 Effects of gradient index on the dimension frequency (Re(Ω)) versus dimension flow velocity

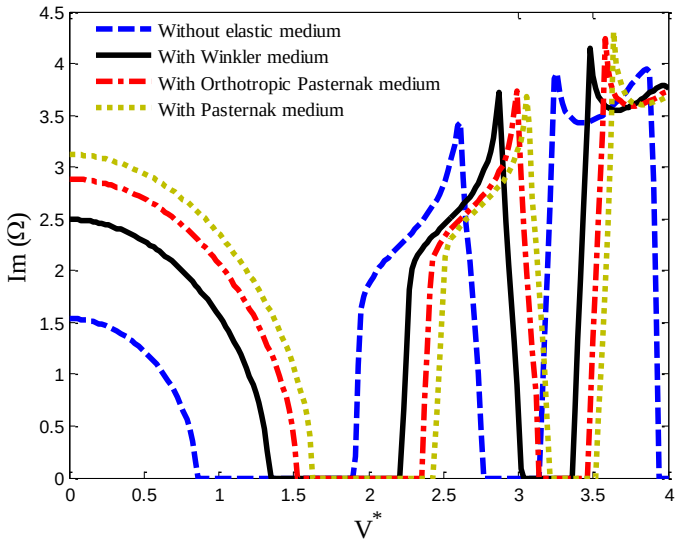

Fig. 6 Effects of elastic medium on the dimension frequency (Im(Ω)) versus dimension flow velocity

metal, show that both mass and stiffness are contributing factors in increasing the value of frequency. Noted that FGMs are ultrahigh temperature-resistant materials suitable for aerospace applications such as aircraft, space vehicles, barrier coating and propulsion systems (Fazzolari and Carrera 2014). Hence, presented results indicate that the FG gradient index has a significant influence on the vibration and instability behaviors of the FGM pipe and should therefore be considered in its optimum design.

The dimensionless frequency and damping of the FG pipe are demonstrated in Figs. 6 and 7 for different temperature-dependent mediums. In this figure, four cases are considered as follows:

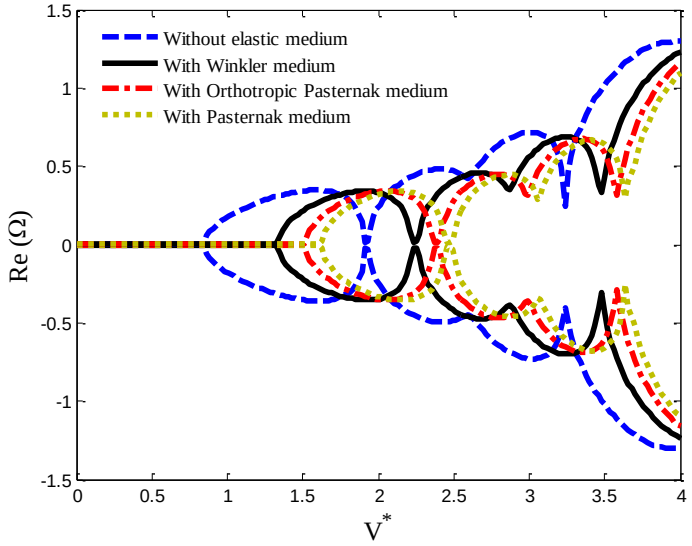

Fig. 7 Effects of elastic medium on the dimension frequency (Re(Ω)) versus dimension flow velocity

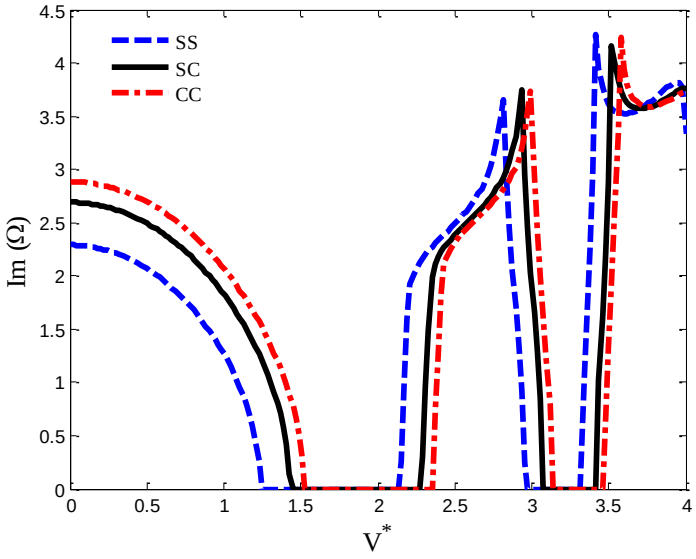

Fig. 8 Effects of boundary conditions on the dimension frequency (Im(Ω)) versus dimension flow velocity

Case 1: $K_W = 0\ N/m^3, K_{g\xi} = 0\ N/m, K_{g\eta} = 0\ N/m \rightarrow$ indicating without elastic medium.

Case 2: $K_W = 41.4\ N/m^3, K_{g\xi} = 0\ N/m, K_{g\eta} = 0\ N/m \rightarrow$ indicating Winkler medium.

Case 3: $K_W = 41.4\ N/m^3, K_{g\xi} = 4.14\ N/m, K_{g\eta} = 4.14\ N/m \rightarrow$indicating Pasternak medium.

Case 4: $K_W = 41.4\ N/m^3, K_{g\xi} = 41.4\ N/m,$
$K_{g\eta} = 4.14\ N/m, \theta = 45^0$ →indicating orthotropic Pasternak medium.

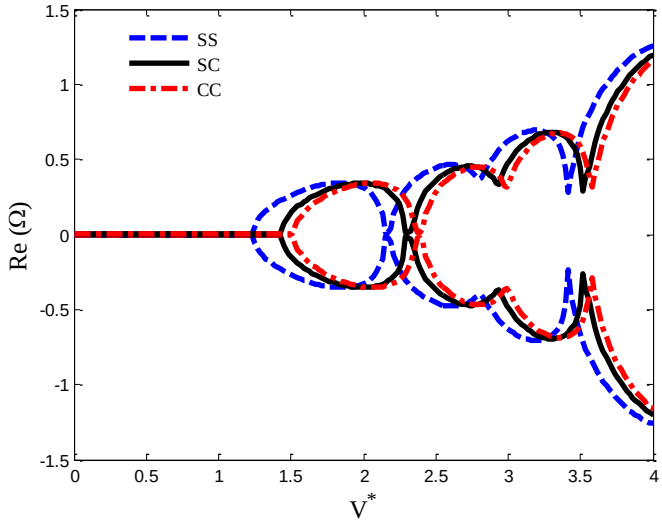

Fig. 9 Effects of boundary conditions on the dimension frequency (Re(Ω)) versus dimension flow velocity

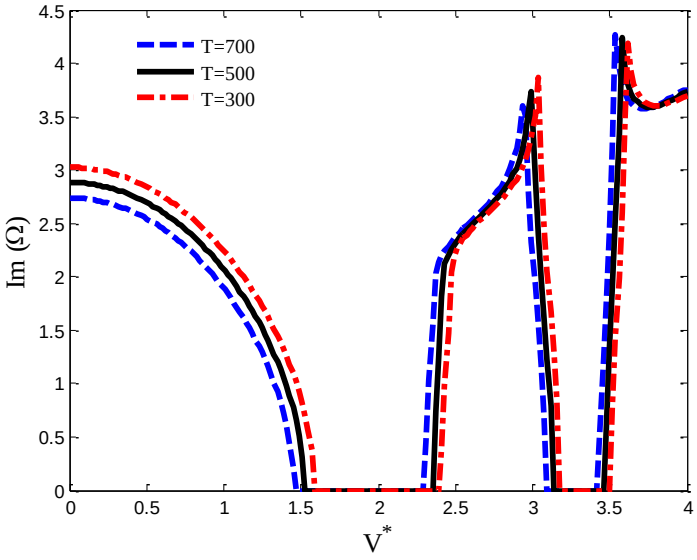

Fig. 10 Effects of temperature gradient on the dimension frequency (Im(Ω)) versus dimension flow velocity

As can be seen, considering elastic medium increases frequency and critical fluid velocity of the FG pipe. It is due to the fact that considering elastic medium leads to stiffer structure. Furthermore, the effect of the Pasternak-type is higher than the Winkler-type on the frequency and critical fluid velocity of the FG pipe. It is perhaps due to the fact that the Winkler-type is capable to describe just normal load of the elastic medium while the Pasternak-type describes both transverse shear and normal loads of the elastic medium. However, we can conclude that the elastic foundation is an important parameter for increasing the stiffness and frequency and delaying in the instability and buckling of pipe.

The effect of the different boundary conditions on the dimensionless frequency and damping of the FG pipe is depicted in Figs. 8 and 9. As can be seen, the frequency and critical fluid velocity of the FG pipe are maximum and minimum for CC and SS boundary conditions, respectively. It is because that considering CC boundary condition leads harder structure.

Figs. 10 and 11 show the dimensionless frequency and damping of the FG pipe for different temperature gradients. It can be also found that the frequency and critical fluid velocity of the FG pipe decrease with increasing temperature which is due to the higher stiffness of FG pipe with lower temperature. Noted that the effect of temperature on the frequency and critical fluid velocity with respect to other parameters presented in this section is lower.

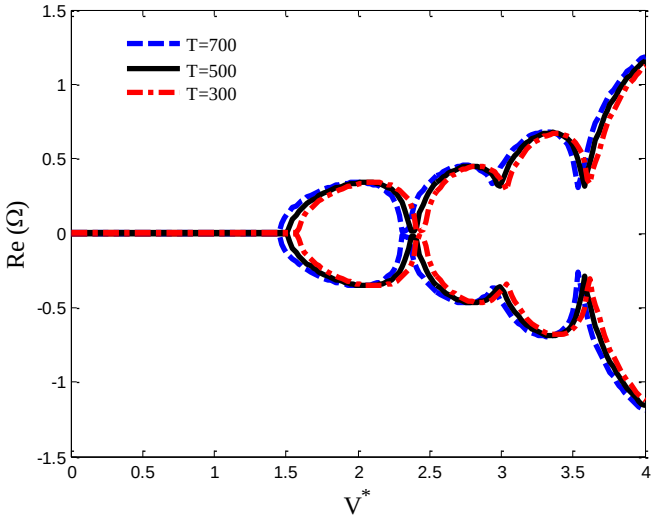

Fig. 11 Effects of temperature gradient on the dimension frequency (Re(Ω)) versus dimension flow velocity

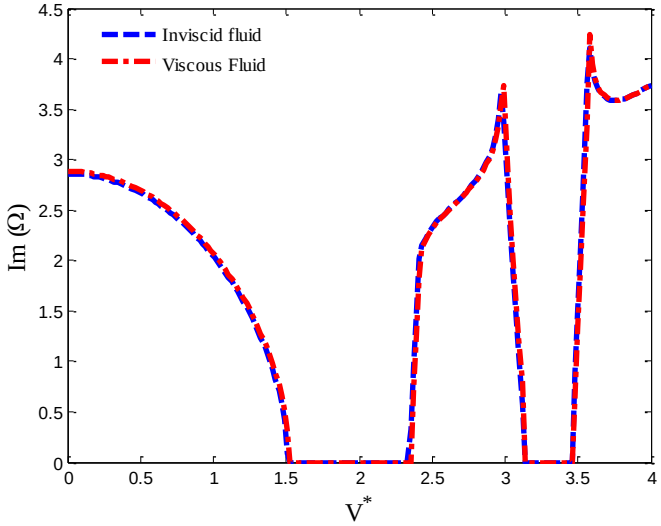

Fig. 12 Effects of fluid viscosity on the dimension frequency (Im(Ω)) versus dimension flow velocity

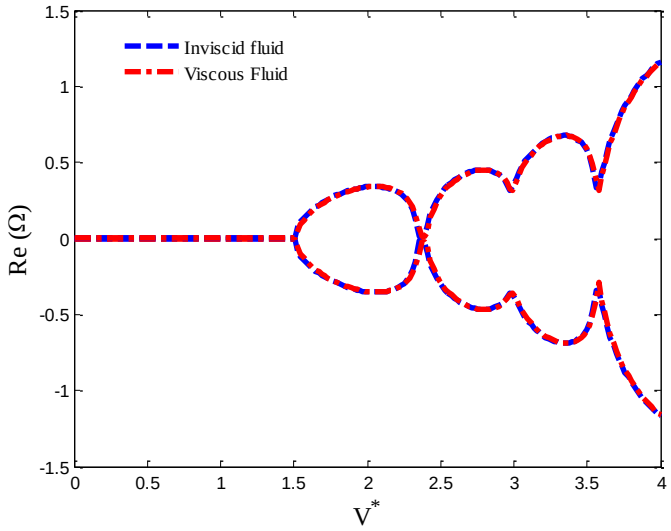

Fig. 13 Effects of fluid viscosity on the dimension frequency (Re(Ω)) versus dimension flow velocity

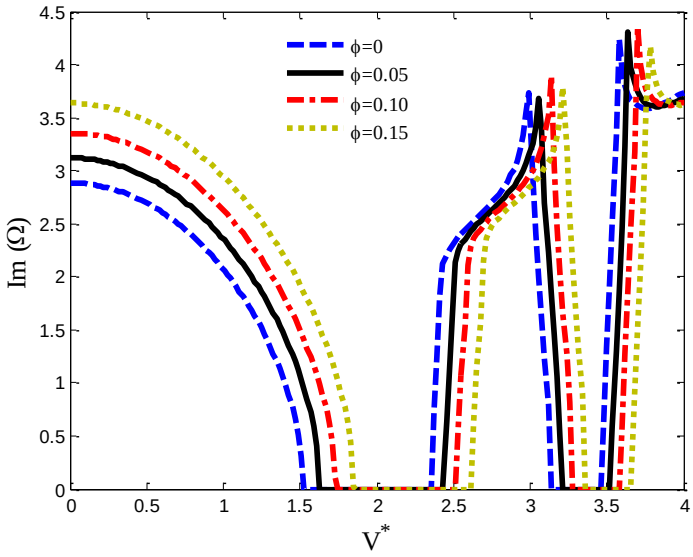

Fig. 14 Effects of nanoparticle volume percent on the dimension frequency (Im(Ω)) versus dimension flow velocity

Figs. 12 and 13 illustrate the effect of fluid viscosity on the Im(Ω) and Re(Ω) of FG pipe versus dimensionless fluid velocity, respectively. The results indicate that viscous fluid increases frequency very little. However, during the flow of a fluid through a FG pipe, the effect of fluid viscosity on the vibration and instability of structure may be ignored. It should be noted that, this is the same as observations made by Wang and Ni (2009).

For presenting the effect of nanoparticle volume fraction in fluid, Figs. 14 and 15 are plotted. As can be seen, with increasing volume fraction of nanoparticles in fluid, the frequency and

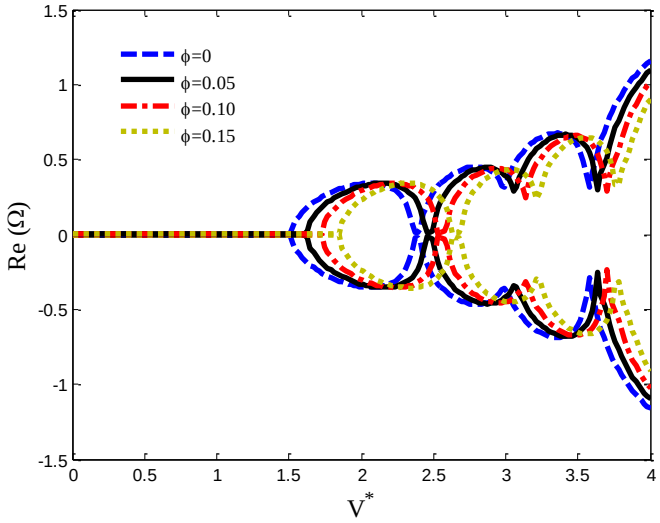

Fig. 15 Effects of nanoparticle volume percent on the dimension frequency (Re(Ω)) versus dimension flow velocity

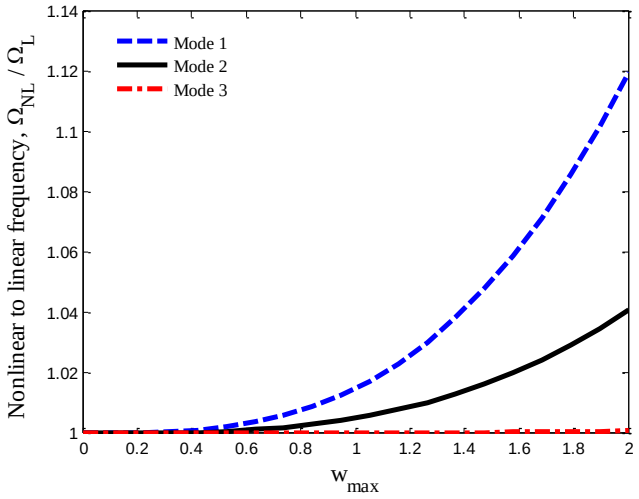

Fig. 16 Nonlinear to linear frequency versus maximum amplitude for different FG gradient index and boundary conditions

critical fluid velocity increase. It is due to the fact that with increasing volume fraction of nanoparticles in fluid, the velocity of fluid decreases and consequently the stability of system increases.

Nonlinear to linear frequency (Ω_{NL}/Ω_L) versus maximum amplitude ($w_{\max}$) for different FG gradient index and boundary conditions is demonstrated in Fig. 16. As can be seen, increasing amplitude, the effect of nonlinear terms in motion equations increases. Furthermore, with increasing FG gradient index, the frequency ratio increases. Meanwhile, considering CC boundary condition decreases frequency ratio. In conclusion, considering pipe with FG gradient index zero

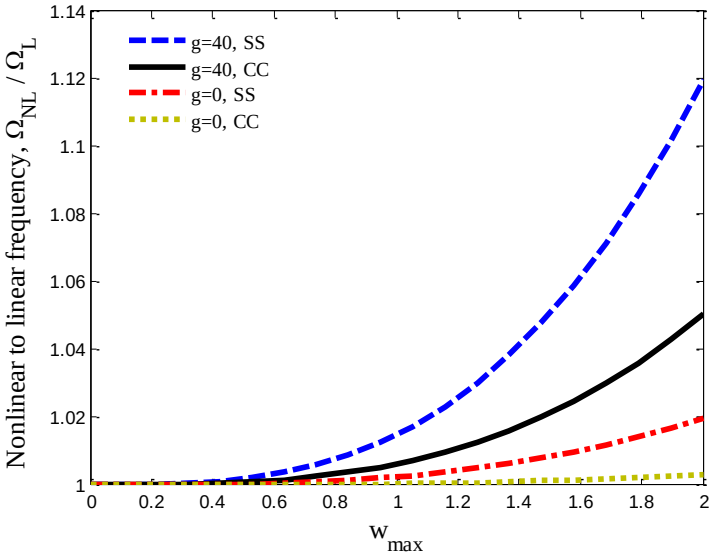

Fig. 17 Nonlinear to linear frequency versus maximum amplitude for different mode numbers

and CC boundary condition, the frequency ratio decreases and consequently, the nonlinear frequency reaches to linear one. However, in the mentioned case, the effect of nonlinear terms in motion equations may be ignored.

Fig. 17 illustrates the Ω_{NL}/Ω_L versus w_{max} for the first three modes of vibration. It can be seen that with increasing mode numbers, the frequency ratio decreases. Hence, the effect of nonlinear terms in motion equations in higher modes can be eliminated.

5. Conclusions

Temperature-dependent nonlinear vibration and instability of FG pipe conveying fluid-nanoparticel mixture were presented in this study. The FG pipe was located in a temperature-dependent elastic medium which was simulated by Pasternak foundation. Based on Reddy shell theory, the motion equations were derived using energy method and Hamilton's principle. GDQM is applied for obtaining the frequency and critical fluid velocity of system so that the effects of the mode numbers, internal fluid velocity, volume percent of nanoparticle in fluid, gradient index, Pasternak medium, temperature, nonlinear terms in motion equations and boundary conditions were considered. Results indicate that fluid velocity plays an important role on the instability of pipe since it can lead to divergence and flutter instabilities. Considering Pasternak medium increases frequency and critical fluid velocity of the FG pipe. Furthermore, with increasing gradient index and decreasing volume percent of nanoparticle in fluid, the frequency and critical fluid velocity of the FG pipe decrease. In addition, the frequency and critical fluid velocity of the FG pipe decrease with increasing temperature gradient. Meanwhile, considering CC boundary condition, higher vibration modes and decreasing FG gradient index, the effect of nonlinear terms in motion equations may be ignored. The results of this study were validated as far as possible by Shen (2003), Pradyumna and Bandyopadhyay (2008), Neves *et al*. (2013), Fazzolari and Erasmo

Carrera (2014). Finally, it is hoped that the results presented in this paper would be helpful for study and design of pipes conveying fluid with applications in oil pipelines, heat exchangers, nuclear reactor components and pump discharge lines.

Acknowledgments

The author would like to thank the reviewers for their comments and suggestions to improve the clarity of this article. They would also like to thank the Isfahan Province Gas Company for their financial support.

References

Abdollahian, M., Ghorbanpour Arani, A., Mosallaie Barzoki, A.A., Kolahchi, R. and Loghman, (2013), "A. Non-local wave propagation in embedded armchair TWBNNTs conveying viscous fluid using DQM", *Physica B*, **418**, 1-15.

Amabili, M., Pellicano, F. and Paidoussis, M.P. (2002), "Non-linear dynamics and stability of circular cylindrical shells conveying flowing fluid", *Comput. Struct.*, **80**, 899-906.

Amabili, M. (2003), "A comparison of shell theories for large-amplitude vibrations of circular cylindrical shells: Lagrangian approach", *J. Sound Vib.*, **264**, 1091-1125.

Amabili, M., Karagiozis, K. and Paidoussis, M.P. (2009), "Effect of geometric imperfections on non-linear stability of circular cylindrical shells conveying fluid", *Int. J. Nonlin. Mech.*, **44**, 276- 289.

Fazzolari, F.A. and Carrera, E. (2014), "Refined hierarchical kinematics quasi-3D Ritz models for free vibration analysis of doubly curved FGM shells and sandwich shells with FGM core", *J. Sound. Vib.*, **333**,1485-1508.

Ghorbanpour Arani, A., Karimi, M.S. and Rabani Bidgoli, M. (2016), "Nonlinear vibration and instability of rotating piezoelectric nanocomposite sandwich cylindrical shells containing axially flowing and rotating fluid-particle mixture", *Polym. Compos.*, doi: 10.1002/pc.23949. (in Press)

Jansen, E.L. (2008), "A perturbation method for nonlinear vibrations of imperfect structures: Application to cylindrical shell vibrations", *Int. J. Solid. Struct.*, **45**, 1124-1145.

Jung, W.Y., Park, W.T. and Han, S.C. (2014), "Bending and vibration analysis of S-FGM microplates embedded in Pasternak elastic medium using the modified couple stress theory", *Int. J. Mech. Sci.*, **87**, 150-162.

Karagiozis, K.N., Amabili, M., Paı¨doussis, M.P. and Misra, A.K. (2005), "Nonlinear vibrations of fluid-filled clamped circular cylindrical shells", *J. Fluid. Struct.*, **21**, 579-595.

Khadimallaha, M.A., Casimir, J.B., Chafra, M. and Smaoui, H. (2011), "Dynamic stiffness matrix of an axisymmetric shell and response to harmonic distributed loads", *Comput. Struct.*, **89**, 467-475.

Khalili, S.M.R., Davar, A. and Malekzadeh Fard, K. (2012), "Free vibration analysis of homogeneous isotropic circular cylindrical shells based on a new three-dimensional refined higher-order theory", *Int. J. Mech. Sci.*, **56**, 1-25.

Kim, Y.W. (2015), Free vibration analysis of FGM cylindrical shell partially resting on Pasternak elastic foundation with an oblique edge", *Compos. Part B: Eng.*, **70**, 263-276.

Kolahchi, R., Moniri Bidgoli, A.M. and Heydari M.M. (2015a), "Size-dependent bending analysis of FGM nano-sinusoidal plates resting on orthotropic elastic medium", *Struct. Eng. Mech.*, **55**, 1001-1014.

Kolahchi, R., Rabani Bidgoli, M. Beygipoor, Gh. and Fakhar, M.H. (2015b), "A nonlocal nonlinear analysis for buckling in embedded FG-SWCNT-reinforced microplates subjected to magnetic field", *J. Mech. Sci. Tech.*, **29**(9), 3669-3677.

Kolahchi, R. and Moniribidgoli, A.M. (2016), "Size-dependent sinusoidal beam model for dynamic

instability of single-walled carbon nanotubes", *Appl. Math. Mech.*, **37**, 265-274.
Kutlu, A. and Omurtag, M.H. (2012), "Large deflection bending analysis of elliptic plates on orthotropic elastic foundation with mixed finite element method", *Int. J. Mech. Sci.*, **65**, 64-74.
Lei, Z.X., Zhang, L.W., Liew, K.M. and Yu, J.L. (2014), "Dynamic stability analysis of carbonnanotube-reinforced functionally graded cylindrical panels using the element-free kp-Ritz method", *Compos. Struct.*, **113**, 328-338.
Liew, K.M., Lei, Z.X., Yu, J.L. and Zhang, L.W. (2014), "Postbuckling of carbon nanotube-reinforced functionally graded cylindrical panels under axial compression using a meshless approach", *Comput. Meth. Appl. Mech. Eng.*, **268**, 1-17.
Mirzavand, B. and Eslami, M.R. (2011), "A closed-form solution for thermal buckling of piezoelectric FGM rectangular plates with temperature-dependent properties", *Acta Mech.*, **218**, 87-101.
Neves, A.M.A., Ferreira, A.J.M., Carrera, E., Cinefra, M., Roque, C.M.C., Jorge, R.M.N. and Soares, C.M.M. (2013), "Free vibration of functionally graded shells by a higherorder shear deformation theory and radial basis functions collocation, accounting for through-the-thickness deformations", *Euro. J. Mech. A/Solid.*, **37**, 24-34.
Ng, T.Y., Lam, Y.K., Liew, K.M. and Reddy J.N. (2001), "Dynamic stability analysis of functionally graded cylindrical shells under periodic axial loading", *Int. J. Solid. Struct.*, **38**, 1295-1300.
Nguyen, D. and Thang, P.T. (2015), "Nonlinear dynamic response and vibration of shear deformable imperfect eccentrically stiffened S-FGM circular cylindrical shells surrounded on elastic foundations", *Aero. Sci. Tech.*, **40**, 115-127.
Pellicano, F. and Avramov K.V. (2007), "Linear and nonlinear dynamics of a circular cylindrical shell connected to a rigid disk", *Commun. Nonlin. Sci. Num. Simul.*, **12**, 496-518.
Pradyumna, S. and Bandyopadhyay, J.N. (2008), "Free vibration analysis of functionally graded curved panels using a higher-order finite element formulation", *J. Sound Vib.*, **318**, 176-192.
Reddy, J.N. (1984), "A Simple Higher Order Theory for Laminated Composite Plates", *J. Appl. Mech.*, **51**, 745-752.
Reddy, J.N. and Praveen, G.N. (1998), "Nonlinear transient thermoelastic analysis of functionally graded ceramic-metal plate", *Int. J. Solid. Struct.*, **35**, 4457-4476.
Shahba, A. and Rajasekaran, S. (2012), "Free vibration and stability of tapered Euler-Bernoulli beams made of axially functionally graded materials", *Appl. Math. Model.*, **36**, 3094-3111.
Shen, H.Sh. and Zhang, Ch.L. (2011), "Nonlocal beam model for nonlinear analysis of carbon nanotubes on elastomeric substrates", *Computat. Mater. Sci.*, **50**, 1022-1029.
Sheng, G.G. and Wang, X. (2009a), "Active control of functionally graded laminated cylindrical shells", *Compos. Struct.*, **90**, 448-457.
Sheng, G.G. and Wang, X. (2009b), "Studies on dynamic behavior of functionally graded cylindrical shells with PZT layers under moving loads", *J. Sound Vib.*, **323**, 772-789 .
Sheng, G.G. and Wang, X. (2010), "Dynamic characteristics of fluid-conveying functionally graded cylindrical shells under mechanical and thermal loads", *Compos. Struct.*, **93**, 162-170.
Shu, C., Chen, W., Xue, H. and Du, H. (2001), "Numerical study of grid distribution effects on accuracy of DQ analysis of beams and plates by error estimation of derivative approximation", *Int. J. Numer. Meth. Eng.*, **51**, 159-179.
Wang, L. and Ni, Q. (2009), "A reappraisal of the computational modelling of carbon nanotubes conveying viscous fluid", *Mech. Res. Commun.*, **36**, 833-837.
Wattanasakulpong, N., Gangadhara Prusty, B., Kelly, D.W. and Hoffman, M. (2012), "Free vibration analysis of layered functionally graded beams with experimental validation", *Mater. Des.*, **36**, 182-190.
Xing, Y., Liu, B. and Xu, T. (2013), "Exact solutions for free vibration of circular cylindrical shells with classical boundary conditions", *Int. J. Mech. Sci.*, **75**, 178-188.
Yang, J. and Shen, H.S. (2003), "Free vibration and parametric resonance of shear deformable functionally graded cylindrical panels", *J. Sound Vib.*, **261**, 871-893.
Zhang, L.W., Lei, Z.X., Liew, K.M. and Yu, J.L. (2014a), "Large deflection geometrically nonlinear analysis of carbon nanotube-reinforced functionally graded cylindrical panels", *Comput. Meth. Appl. Mech. Eng.*,

273, 1-18.
Zhang, L.W., Lei, Z.X., Liew, K.M. and Yu, J.L. (2014b), "Static and dynamic of carbon nanotube reinforced functionally graded cylindrical panels", *Compos. Struct.*, **111**, 205-212.

CC